

ORBITAL EVOLUTION IN BINARY AND TRIPLE STARS, WITH AN APPLICATION TO SS LACERTAE

PETER P. EGGLETON^{1,2} AND LUDMILA KISELEVA-EGGLETON^{1,3}

Received 2000 November 29; accepted 2001 August 3

ABSTRACT

We present equations governing the way in which both the orbit and the intrinsic spins of stars in a close binary should evolve subject to a number of perturbing forces, including the effect of a third body in a possibly inclined wider orbit. We illustrate the solutions in some binary star and triple star situations: tidal friction in a wide but eccentric orbit of a radio pulsar about a B star (0045–7319), the Darwin and eccentricity instabilities in a more massive but shorter period massive X-ray binary, and the interaction of tidal friction with Kozai cycles in a triple star, such as β Per at an early stage in that star's life, when all three components were zero-age main sequence stars. We also attempt to model in some detail the interesting triple system SS Lac, which stopped eclipsing in about 1950. We find that our model of SS Lac is quite constrained by the relatively good observational data of this system and leads to a specific inclination (29°) of the outer orbit relative to the inner orbit at epoch zero (1912). We make some predictions about changes to system parameters in the short term (20–40 yr) and also in the medium term (up to ~ 3000 yr). Although the intrinsic spins of the stars have little effect on the orbit, the converse is not true: the spin axes can vary their orientation relative to the close binary by up to 120° on a timescale of about a century.

Subject headings: binaries: general — celestial mechanics — stars: evolution — stars: individual (SS Lacertae)

1. INTRODUCTION

We model the effect on a short-period binary star orbit, and also on the spins of the two components, of the following perturbations:

1. A third body (treated as a point mass) in a longer period orbit.
2. The quadrupolar distortion of the stars due to their intrinsic spin.
3. The further quadrupolar distortion due to their mutual gravity.
4. Tidal friction, in the equilibrium-tide approximation.
5. General relativity.

The third body's effect is treated only at the quadrupole level of approximation, although in principle it should not be difficult to go to a higher order if necessary. The stellar distortion terms are also treated only at the quadrupole level; it might be rather more difficult here to go to a higher order, but it is probably even less necessary. Each of the perturbing forces has been averaged over an approximately Keplerian orbit. We follow the analysis of Eggleton, Kiseleva, & Hut (1998; hereafter EKH98) for effects 2–4. The third-body perturbation comes from the same type of analysis (as does the familiar Schwarzschild-metric correction).

We illustrate the model with some binary and triple examples:

1. The circularization of an initially eccentric orbit of a neutron star (NS) around an obliquely rotating massive normal B star, based on the SMC radio pulsar 0045–7319 (Kaspi et al. 1994); we assume that the B star has a spin inclined at a large angle (135°) to the orbit and model the way in which the spin parallelizes as well as pseudosynchronizes with the orbit.
2. The Darwin instability, i.e., the tendency for an orbit to desynchronize if the spin angular momentum of a star is more than a third of the orbital angular momentum, and the eccentricity instability, in which rapid enough prograde rotation of the star causes the eccentricity to increase.
3. Kozai cycles, i.e., cyclic large-amplitude variation of the eccentricity of the inner binary due to a highly inclined outer orbit, which, in combination with tidal friction, can make the inner orbit shrink, even if it is initially too wide for tidal friction to be important.

We base some of these illustrations on actual stellar systems, but the data on these systems are not (yet) sufficient to test the model rigorously.

¹ Lawrence Livermore National Laboratory, Institute of Geophysics and Planetary Physics, P.O. Box 808, L-413, Livermore, CA 94550; ppe@igpp.ucllnl.org, lkisseleva@igpp.ucllnl.org.

² On leave from the Institute of Astronomy, Madingley Road, University of Cambridge, Cambridge CB3 0HA, UK.

³ Now at School of Science, Saint Mary's College, P.O. Box 3517, Moraga, CA 94575.

We then apply the model to the interesting 14.4 day binary SS Lac, which eclipsed for the first 50 yr of the 20th century and stopped eclipsing later. Recently, Torres & Stefanik (2000; hereafter TS00) have demonstrated the existence of a third body in a ~ 700 day orbit, which, if inclined at a suitable angle to the inner orbit, could well account for the necessary change in the orientation of the orbit relative to the observer. We find that in order to accommodate the data given by TS00, we require the outer orbit to be inclined at about 29° (or 151°) to the inner orbit. We also require a specific value (37°) for the longitude of the outer orbit's axis relative to the inner orbital frame in 1912 (epoch zero). We find a modest variation with time in the eccentricity and in the rate of change of inclination of the inner orbit to the line of sight. These cause us to revise slightly the masses found by TS00. Our model is fully constrained by the known data on this system, but it is not overconstrained, so that unfortunately we are not in a position to confirm that the model is correct. We can, however, make predictions for changes that should be capable of confirmation or refutation in about 20 yr.

In § 2 we set out the equations governing the change in the orbit (and also in the rates of rotation of the two components), discussing the level of approximation that we use. In § 3 we illustrate the behavior of the equations in a number of straightforward cases, two without and one with a third body. In § 4 we apply our model to SS Lac, and we conclude with a discussion in § 5. Some mathematical details are given in the Appendix.

2. EQUATIONS FOR ORBITAL EVOLUTION

The evolution of the orbit under the influence of the perturbations listed in § 1 is well expressed in terms of the following five vectors: e , the Laplace-Runge-Lenz vector, which points along the major axis in the direction of periastron and has magnitude e , the eccentricity; h , the orbital angular momentum vector, pointing perpendicular to the orbital plane and with magnitude h , the orbital angular momentum per unit reduced mass μ ; $q \equiv h \times e$, which makes a right-handed orthogonal triad e, q, h with the previous two vectors, since e and h are always mutually perpendicular; and also the spin vectors Ω_1 and Ω_2 of the two components. The vector q is along the latus rectum, the line through the focus parallel to the minor axis. It is also convenient to define unit vectors $\hat{e}, \hat{q}, \hat{h}$, a right-handed orthogonal unit basis. This basis is not an inertial frame, of course, since it varies with time as the system evolves under the perturbations. However, provided that the perturbations are sufficiently small that they do not affect the orbit by more than a small amount on timescales less than the period of the outer orbit, it is possible to estimate rather simply the rates of change of these five vectors in response to the five perturbative forces listed above.

The equations governing the rates of change of e, h, Ω_1 , and Ω_2 were derived by EKH98, but note that five equations in that paper were affected by a mistaken factor of 2. The mistaken equations are identified in the Appendix to the present paper, and the equations presented here include the correction. We are grateful to R. Mardling (2000, private communication) for pointing this out. Independently, our definition of the tidal-friction timescale t_F in this paper differs by a factor of 2 from that of t_{TF} in EKH98.

The equations can be written as

$$\frac{1}{e} \frac{de}{dt} = (Z_1 + Z_2 + Z_{GR})\hat{q} - (Y_1 + Y_2)\hat{h} - (V_1 + V_2)\hat{e} - (1 - e^2)[5S_{eq}\hat{e} - (4S_{ee} - S_{qq})\hat{q} + S_{qh}\hat{h}], \quad (1)$$

$$\frac{1}{h} \frac{dh}{dt} = (Y_1 + Y_2)\hat{e} - (X_1 + X_2)\hat{q} - (W_1 + W_2)\hat{h} + (1 - e^2)S_{qh}\hat{e} - (4e^2 + 1)S_{eh}\hat{q} + 5e^2S_{eq}\hat{h}, \quad (2)$$

$$I_1 \frac{d\Omega_1}{dt} = \mu h(-Y_1\hat{e} + X_1\hat{q} + W_1\hat{h}), \quad (3)$$

$$I_2 \frac{d\Omega_2}{dt} = \mu h(-Y_2\hat{e} + X_2\hat{q} + W_2\hat{h}). \quad (4)$$

An equation for q follows from differentiating the product $q = h \times e$. The quantities V_i, W_i, X_i, Y_i , and Z_i , one for each component of the inner pair, are given below. They arise from the quadrupolar distortion of the two components. The first two are dissipative terms due to tidal friction, which tend to enforce orbital circularization and synchronous rotation, at least in the absence of a third-body perturbation. The next three are mainly nondissipative perturbations due to quadrupole distortions, giving precession and apsidal motion, but X and Y do contain a small dissipative contribution that tends to bring the stellar rotations into parallel with the orbit. The Z term, giving apsidal motion, contains a general relativity (GR) correction. The tensor S , with components S_{ee}, S_{eq}, \dots in the e, q, h frame, is due only to the third body, and its components are also given somewhat further below, in equations (15) and (16).

The dissipative terms V_1 and W_1 are

$$V_1 = \frac{9}{t_{F1}} \left[\frac{1 + (15/4)e^2 + (15/8)e^4 + (5/64)e^6}{(1 - e^2)^{13/2}} - \frac{11\Omega_{1h}}{18\omega} \frac{1 + (3/2)e^2 + (1/8)e^4}{(1 - e^2)^5} \right], \quad (5)$$

$$W_1 = \frac{1}{t_{F1}} \left[\frac{1 + (15/2)e^2 + (45/8)e^4 + (5/16)e^6}{(1 - e^2)^{13/2}} - \frac{\Omega_{1h}}{\omega} \frac{1 + 3e^2 + (3/8)e^4}{(1 - e^2)^5} \right], \quad (6)$$

with similar expressions for star 2. The term $\Omega_{1h} \equiv \Omega_1 \cdot \hat{h}$ is the component of Ω_1 in the direction of \hat{h} , i.e., parallel to the orbital axis, and ω is the mean angular velocity of the inner orbit, i.e., $2\pi/P$. The tidal-friction timescale t_F is estimated here, in terms of an inherent viscous timescale t_V for each star, as

$$\frac{1}{t_{F1}} = \frac{9}{t_{V1}} \frac{R_1^8}{a^8} \frac{MM_2}{M_1^2} \frac{1}{(1-Q_1)^2}. \quad (7)$$

The terms M_1 and M_2 are the masses of the two components of the inner binary, M their sum, R_1 and R_2 their radii, and a the semimajor axis. The term Q_1 is a coefficient measuring the quadrupolar deformability of the star; it is closely related to the apsidal motion constant (EKH98). For an $n \sim 3$ polytrope,

$$I = 0.08MR^2, \quad Q = 0.028. \quad (8)$$

The intrinsic viscous timescale of the star, t_{V1} , is not easily determined, but we use an estimate based on (1) the timescale on which the star would be turned over if most of the luminosity L_1 were carried by convection (Zahn 1977) and (2) a dimensionless factor γ , which comes from integrating over the star the rate-of-strain tensor (squared) of the time-dependent tidal velocity field:

$$\frac{1}{t_{V1}} = \gamma_1 \left(\frac{L_1}{3M_1 R_1^2} \right)^{1/3}, \quad \gamma_1 \sim 0.01. \quad (9)$$

The timescale t_{V1} is of the order of years or decades. The quantity γ (see the Appendix) is determined by a model of the tidal amplitude as a function of radius through the star (EKH98), obtained by solving explicitly the velocity field required by the continuity equation if isobaric surfaces within the star are always to be equipotential surfaces—the basic assumption of the equilibrium-tide model.

The contributions X_1 , Y_1 , and Z_1 to the rotation of the axes due to rotational and tidal distortion of star 1 (including the small contribution of tidal friction) are given by

$$X_1 = -\frac{M_2 A_1}{2\mu\omega a^5} \frac{\Omega_{1h}\Omega_{1e}}{(1-e^2)^2} - \frac{\Omega_{1q}}{2\omega t_{F1}} \frac{1 + (9/2)e^2 + (5/8)e^4}{(1-e^2)^5}, \quad (10)$$

$$Y_1 = -\frac{M_2 A_1}{2\mu\omega a^5} \frac{\Omega_{1h}\Omega_{1q}}{(1-e^2)^2} + \frac{\Omega_{1e}}{2\omega t_{F1}} \frac{1 + (3/2)e^2 + (1/8)e^4}{(1-e^2)^5}, \quad (11)$$

$$Z_1 = \frac{M_2 A_1}{2\mu\omega a^5} \left[\frac{2\Omega_{1h}^2 - \Omega_{1e}^2 - \Omega_{1q}^2}{2(1-e^2)^2} + \frac{15GM_2}{a^3} \frac{1 + (3/2)e^2 + (1/8)e^4}{(1-e^2)^5} \right]. \quad (12)$$

Here μ is the reduced mass, and Ω_{1e} and Ω_{1q} are the components of Ω_1 in the directions of \hat{e} and \hat{q} . EKH98 give the linear combinations $X_1\Omega_{1q} - Y_1\Omega_{1e}$ and $X_1\Omega_{1e} + Y_1\Omega_{1q}$ rather than X_1 and Y_1 directly: see the Appendix to this paper. The coefficient A_1 is

$$A_1 = \frac{R_1^5 Q_1}{1 - Q_1}. \quad (13)$$

In all of equations (5)–(13), we exchange subscript 1 for subscript 2 to find the corresponding term for the second component of the inner binary.

The GR contribution to apsidal motion is

$$Z_{GR} = \frac{3GM\omega}{ac^2(1-e^2)}. \quad (14)$$

The effect of a third body (mass M_3) is included here only at the quadrupole level of approximation, following Kiseleva, Eggleton, & Mikkola 1998 (hereafter KEM98). At this level, the center of gravity (CG) of the inner binary and the third body are unperturbed, and so the outer orbit is exactly constant. Like the inner orbit, it can be described by a right-handed triad $\mathbf{E}, \mathbf{Q}, \mathbf{H}$. Within the inner binary, there is a perturbative force that in the lowest approximation is linear in the vector separation: $\delta f_i \propto T_{ij} d_j$, where \mathbf{d} is the separation of the inner pair. The tensor T depends on \mathbf{D} , the separation of the outer pair (i.e., of the third body and the CG of the inner pair). Averaging T over an outer orbit and then averaging the effect of δf over the inner orbit, assuming that *both* orbits are only slowly varying on this timescale, we find that the tensor S of equations (1) and (2) is

$$S_{ij} = C(\delta_{ij} - 3\hat{H}_i \hat{H}_j), \quad C = \frac{M_3 \omega_{out}^2}{4(M + M_3)\omega(1-e^2)^{1/2}(1-e_{out}^2)^{3/2}}. \quad (15)$$

The term $|\mathbf{E}| \equiv e_{out}$ is the eccentricity of the outer orbit, and ω_{out} is the outer orbital frequency. Then, the effect of the force δf on the vectors \mathbf{e} and \mathbf{h} are as indicated in equations (1)–(2), where on referring to the basis vectors $\mathbf{e}, \mathbf{q}, \mathbf{h}$, we have

$$S_{ee} = C(1 - 3\hat{H}_e \hat{H}_e), \quad S_{eq} = -3C\hat{H}_e \hat{H}_q, \quad \text{etc.} \quad (16)$$

A somewhat surprising but welcome simplification is that after averaging T over D , we have dependence only on H , and not on E and Q as well. Note that C is *not* a constant, because of its dependence on e .

Equations (1)–(4) are closed by the fact that a and ω , which appear in several places on the right-hand sides, are obtained in terms of e and h by way of the relations

$$a = \frac{h^2}{GM(1 - e^2)}, \quad \omega^2 = \left(\frac{2\pi}{P}\right)^2 = \frac{GM}{a^3}. \quad (17)$$

As \hat{e} and \hat{h} evolve away from their initial values, along with Ω_1 and Ω_2 , we have to compute various vector and scalar products: $\mathbf{q} = \mathbf{h} \times \mathbf{e}$, Ω_e , Ω_q , \hat{H}_e , etc.

The physical significance of V , W , X , Y , and Z is perhaps most easily seen by splitting each of the equations (1) and (2) into two pieces, one each for the moduli (e , h) and one each for the unit vectors \hat{e} , \hat{h} :

$$\frac{1}{e} \frac{de}{dt} = -V_1 - V_2 - 5(1 - e^2)S_{eq}, \quad (18)$$

$$\frac{d\hat{e}}{dt} = [Z_1 + Z_2 + Z_{GR} + (1 - e^2)(4S_{ee} - S_{qq})]\hat{\mathbf{q}} - [Y_1 + Y_2 + (1 - e^2)S_{qh}]\hat{\mathbf{h}}, \quad (19)$$

$$\frac{1}{h} \frac{dh}{dt} = -W_1 - W_2 + 5e^2S_{eq}, \quad (20)$$

$$\frac{d\hat{h}}{dt} = [Y_1 + Y_2 + (1 - e^2)S_{qh}]\hat{e} - [X_1 + X_2 + (4e^2 + 1)S_{eh}]\hat{\mathbf{q}}. \quad (21)$$

Equations (19) and (21) can both be written as

$$\frac{d\hat{\mathbf{u}}}{dt} = \mathbf{K} \times \hat{\mathbf{u}}, \quad (22)$$

$$\mathbf{K} = (X_1 + X_2 + X_{TB}, Y_1 + Y_2 + Y_{TB}, Z_1 + Z_2 + Z_{GR} + Z_{TB}). \quad (23)$$

Clearly, $\mathbf{K} \equiv (X, Y, Z) \equiv X\hat{e} + Y\hat{\mathbf{q}} + Z\hat{h}$ is the angular velocity of the e , q , h frame relative to an inertial frame. The terms with suffix TB arise from the third body, and can be readily identified with the corresponding S -terms in equations (19) and (21). It is easy to see that $\hat{\mathbf{q}}$ satisfies the same equation (22) as \hat{e} and \hat{h} .

Equations (1)–(4) can be integrated numerically, using, for example, a four-stage Runge-Kutta procedure. However, equation (1) as it stands has the slight problem, numerically, that in situations in which $e \rightarrow 0$ (usually as a result of tidal friction), \hat{e} becomes undefined. This is easily solved by using instead equations (18) and (19). There is, of course, some redundancy in the \hat{e} equation, but equations (18) and (19) together are very well behaved. There is not the same problem with equation (2), since h can hardly get to zero in realistic circumstances. Consequently, equations (2)–(4), with (18) and (19), i.e., 13 first-order ordinary differential equations in all, are quite readily integrated numerically as they stand. There are, in fact, two redundancies, since $\hat{e} \cdot \mathbf{h} = 0$, as well as $\hat{e} \cdot \hat{e} = 1$.

We find it convenient to use as our computational (and inertial) frame the *initial* ($t = 0$) orbital frame, i.e. \hat{e}_0 , $\hat{\mathbf{q}}_0$, \hat{h}_0 . We need to be given a number of constant scalars and vectors, i.e., M_i , R_i , L_i , I_i , and Q_i for each of the inner pair of stars, and M_3 , H , and e_{out} for the third body and outer orbit. We also have to supply 12 initial values for e , h , Ω_1 , and Ω_2 . Some of the components are rather trivial, because by the above definition, $\hat{e}_0 = (1, 0, 0)$ and $\hat{h}_0 = (0, 0, 1)$ at $t = 0$, and of course, $\hat{\mathbf{q}}_0 = (0, 1, 0)$. The quantities a and ω at $t = 0$ follow from e and h at $t = 0$ by equations (17).

The nontrivial initial vectors H , Ω_1 , and Ω_2 are all given directions in the obvious spherical-polar form, e.g.,

$$\hat{H} = \sin \alpha_H \cos \beta_H \hat{e} + \sin \alpha_H \sin \beta_H \hat{\mathbf{q}} + \cos \alpha_H \hat{h}. \quad (24)$$

Thus, α_H and β_H are two of the three polar coordinates, the colatitude and longitude, of the vector \hat{H} in the orbital frame. We view H as a vector starting at the focus, and intersecting a sphere that is centered on the focus and has north pole on the \hat{h} axis. Longitude zero (on the equator) is on the \hat{e} axis, i.e., the projection of periastron. The components of \hat{H} are constant in the computational frame of \hat{e}_0 , $\hat{\mathbf{q}}_0$, \hat{h}_0 , but the components \hat{H}_e , \hat{H}_q , and \hat{H}_h that appear in equations (16) change with time because e , q , and h change with time in the \hat{e}_0 , $\hat{\mathbf{q}}_0$, \hat{h}_0 frame, according to equation (22).

The directions of Ω_1 and Ω_2 are given similarly by pairs of angles α_{Ω_1} , β_{Ω_1} , etc. These angles have to be given initially, but of course the Ω values, unlike H , vary both in the inertial frame and in the instantaneous orbital frame.

In order to be able to determine the radial velocity curve and/or the eclipse light curve, and how they might change with time, we have to specify in addition the (constant) direction \hat{J} from which the orbit is observed—constant (like \hat{H}) in the \hat{e}_0 , $\hat{\mathbf{q}}_0$, \hat{h}_0 frame, but not, of course, in the \hat{e} , $\hat{\mathbf{q}}$, \hat{h} frame. We specify \hat{J} by two angles in the same way as \hat{H} , and call them α_J and β_J . The angle α_J is just the usual inclination of the orbit to the line of sight. The angle β_J is almost the same as the “longitude of periastron.” The latter quantity is usually called ω , but we call it ω_{lp} , since we have already used ω for the orbital frequency. The relation between β_J and ω_{lp} is

$$\beta_J + \omega_{\text{lp}} = 270^\circ. \quad (25)$$

We think of α_J and β_J first as given initial conditions, but at later times, they can be evaluated from

$$\cos \alpha_J = \hat{\mathbf{J}} \cdot \hat{\mathbf{h}}, \quad \tan \beta_J = \frac{\hat{\mathbf{J}} \cdot \hat{\mathbf{q}}}{\hat{\mathbf{J}} \cdot \hat{\mathbf{e}}}. \quad (26)$$

The vector $\hat{\mathbf{J}}$ is a constant in space, but variable in the orbital frame $\hat{\mathbf{e}}, \hat{\mathbf{q}}, \hat{\mathbf{h}}$, since these unit vectors vary with time. The same equations (26), mutatis mutandis, give the corresponding α (colatitude) and β (longitude) for the other vectors, \mathbf{H}, Ω_1 , and Ω_2 , at later times.

If we are fortunate enough to have very accurate observations over sufficiently long stretches of time, we may be able to measure some rates of change, such as \dot{P} , \dot{e} , $\dot{\alpha}_J$, and $\dot{\beta}_J$. Equation (18) already gives \dot{e} , and along with equations (17) and (20), this gives \dot{P} (or $\dot{\omega}$ or \dot{a}):

$$-\frac{\dot{a}}{2a} = \frac{\dot{\omega}}{3\omega} = -\frac{\dot{P}}{3P} = W_1 + W_2 + \frac{(V_1 + V_2)e^2}{1 - e^2}. \quad (27)$$

The third-body terms cancel, since they are conservative and do no work around a Keplerian orbit at our level of approximation: only tidal-friction terms affect P (or a). We can differentiate equations (26) with respect to time, keeping $\hat{\mathbf{J}}$ constant and using equation (22) for any of $\hat{\mathbf{e}}, \hat{\mathbf{q}}, \hat{\mathbf{h}}$:

$$\dot{\alpha}_J = -\frac{\hat{\mathbf{J}} \cdot \mathbf{K} \times \hat{\mathbf{h}}}{|\hat{\mathbf{J}} \times \hat{\mathbf{h}}|}, \quad \dot{\beta}_J = \frac{(\hat{\mathbf{J}} \cdot \hat{\mathbf{h}})(\hat{\mathbf{J}} \cdot \mathbf{K}) - \mathbf{K} \cdot \hat{\mathbf{h}}}{|\hat{\mathbf{J}} \times \hat{\mathbf{h}}|^2}, \quad (28)$$

where \mathbf{K} is the rotation rate of the frame as given in equation (23). The second relation involved some elementary vector manipulations, but the first came directly from equations (22) and (26), using $\sin \alpha_J = |\hat{\mathbf{J}} \times \hat{\mathbf{h}}|$.

We wish to emphasize the following point, which we believe is treated incorrectly in much of the literature that we have read. The rate of rotation of the line of apses, $\dot{\omega}_{\text{lp}} \equiv -\dot{\beta}_J$, is usually attributed to Z , the $\hat{\mathbf{h}}$ component of \mathbf{K} , to the extent that Z is normally referred to as ‘‘apsidal motion.’’ However, it is easy to see that $\dot{\beta}_J$ in equation (28) can be nonzero on account of the $\hat{\mathbf{e}}$ and $\hat{\mathbf{q}}$ components X and Y of \mathbf{K} as well, as will happen with a massive rotating star whose spin axis is highly inclined to the orbital axis and precessing about it. We can see that if $X, Y = 0$, so that $\mathbf{K} = Z\hat{\mathbf{h}}$, then $\dot{\omega}_{\text{lp}} \equiv -\dot{\beta}_J = Z$, as expected. However, if X and Y are not zero (precession), they contribute to $\dot{\beta}_J$, even in the case that $Z = 0$. Note that this effect does not depend in any way on the details of our model: it only depends on the fact that the orbital frame $\mathbf{e}, \mathbf{q}, \mathbf{h}$ has some general angular velocity $\mathbf{K} = X\hat{\mathbf{e}} + Y\hat{\mathbf{q}} + Z\hat{\mathbf{h}}$, while the system is viewed from a fixed direction $\hat{\mathbf{J}}$, with variable colatitude α_J and longitude β_J in the $\mathbf{e}, \mathbf{q}, \mathbf{h}$ frame.

The effect of precession on $\dot{\beta}_J$ is mainly to swing the line of apses back and forward (libration), rather than to advance it monotonically (circulation), as does Z . However, for the case in which (1) Ω is not parallel to $\hat{\mathbf{h}}$, (2) the tidal friction terms in equations (10) and (11) are negligible (which they usually are), and (3) the Ω -dependent term in equation (12) dominates over the remaining term (which is usually the case for rapidly rotating components), the librating and circulating effects are comparable.

Our model can be used to provide times (or phases) of eclipses, when the inclination is sufficient for eclipses to occur. We use the simplest approximation, that the stars are spherical. For the beginning and end of an eclipse, we have to satisfy the equation

$$|\hat{\mathbf{J}} \times \mathbf{d}| = \mathbf{R}_1 + \mathbf{R}_2. \quad (29)$$

Here \mathbf{d} , the vectorial separation of the two stars, has components in the $\hat{\mathbf{e}}, \hat{\mathbf{q}}, \hat{\mathbf{h}}$ frame given by the usual formula,

$$\mathbf{d} = \frac{l}{1 + e \cos \theta} (\hat{\mathbf{e}} \cos \theta + \hat{\mathbf{q}} \sin \theta), \quad (30)$$

with $l = a(1 - e^2) = h^2/GM$ being the semi-latus-rectum. Equations (29) and (30) give a quartic equation for $\cos \theta$, which we solve analytically. The coefficients of the quartic are determined by $\hat{\mathbf{J}} \cdot \hat{\mathbf{e}}$ and $\hat{\mathbf{J}} \cdot \hat{\mathbf{q}}$, which vary with time as the basis set moves. Having determined the four, two, or zero real roots that lie in the range $[-1, 1]$, we can determine the phase Φ (i.e., time divided by period) of ingress and egress from the usual formulae:

$$2\pi\Phi = \psi - \sin \psi, \quad \cos \psi = \frac{e + \cos \theta}{1 + e \cos \theta}. \quad (31)$$

This is phase measured from periastron ($\theta = 0$). We can also determine the phases of other significant points on the orbit. The point where the projection on to the orbital plane of the line-of-sight vector $\hat{\mathbf{J}}$ intersects the orbit (conjunction) is given by $\theta = \theta_1$, where

$$[\hat{\mathbf{J}} - (\hat{\mathbf{J}} \cdot \hat{\mathbf{h}})\hat{\mathbf{h}}] \times \mathbf{d} = 0, \text{ i.e., } \tan \theta_1 = \frac{\hat{\mathbf{J}} \cdot \hat{\mathbf{q}}}{\hat{\mathbf{J}} \cdot \hat{\mathbf{e}}}. \quad (32)$$

The point where the radial component of velocity (relative to the CG) vanishes is given by $\theta = \theta_2$, where

$$\hat{\mathbf{J}} \cdot \dot{\mathbf{d}} = 0, \quad \dot{\mathbf{d}} = \frac{h}{l} [-\hat{\mathbf{e}} \sin \theta + (e + \cos \theta)\hat{\mathbf{q}}], \quad (33)$$

so that

$$\sin(\theta_2 - \theta_1) = e \sin \theta_1. \quad (34)$$

Thus, the values of θ at both of these points are also functions of $\hat{\mathbf{J}} \cdot \hat{\mathbf{e}}$ and $\hat{\mathbf{J}} \cdot \hat{\mathbf{q}}$. There are two values of both θ_1 and θ_2 in the range 0° – 360° ; in § 4 we take θ_1 such that star 1 is in front and θ_2 such that star 1 is behind. For triple systems, we ignore the small effect due to the variable motion of the CG of the inner pair. The points where the radial velocity is a maximum (or minimum) are given by $\hat{\mathbf{J}} \cdot \mathbf{d} = 0$ (since $\dot{\mathbf{d}} \parallel \mathbf{d}$ in the unperturbed orbit), and hence by $\theta_3 = \theta_1 \pm 180^\circ$.

The model we present here has, we believe, the merit of considerable simplicity, both conceptually and numerically. We emphasize here the approximations on which it is based:

1. Only the quadrupolar component of the distortion of each star is modeled. This assumption may be fairly good in systems that are only mildly eccentric, but can be expected to be less valid in systems of high eccentricity. For the distortion due to rotation, it is assumed that the stars are in solid-body rotation.

2. The components are assumed to adjust instantaneously to fill an equipotential of the joint gravitational-centrifugal potential. This leads to a specific tidal velocity field within each star, whose shear, combined with a viscosity assumed to be due to convectively driven turbulence, determines the force of tidal friction. Although some analyses have argued that the effect of convection in a star with a radiative envelope and a convective core is small, we follow the analysis of EKH98, which shows that tidal dissipation within a convective core is not small.

3. The effect of the third body is only modeled at the quadrupole level of approximation. This is sufficient to demonstrate such phenomena as Kozai cycles (Kozai 1962), in which the third body, if placed in an orbit highly inclined to that of the first two, causes large fluctuations in eccentricity on a long timescale. The approximation is not very good for a *parallel* orbit, since all the off-diagonal components of the tensor S vanish, so that the only effect in equations (18)–(21) is the apsidal-motion term. It therefore does not allow us to model the fluctuations in eccentricity that the third body produces in the inner pair; actually, these are quite small, according to an N -body integration, but they can be significant on a long timescale when combined with tidal friction (KEM98).

4. The same level of approximation means that there is no additional force, or couple, on the outer binary. Consequently, angular momentum is not conserved: the inner binary can gain or lose angular momentum, but not the outer. Moderate accuracy relies on the fact that the angular momentum of the outer binary is large compared to the inner, so that a substantial amount lost by the inner counts as only a small perturbation to the outer. However, angular momentum increases with only the cube root of the period at given masses, so that a period ratio of 50 (an unusually small value, but appropriate to SS Lac) means an angular momentum ratio that is not large.

3. SOME ILLUSTRATIVE EXAMPLES

Our model for perturbed orbits is original to the extent that (1) it has a specific formulation for the parallelization of stellar spin that is initially oblique to, or even antiparallel to, orbital angular momentum, and (2) it includes the effect of a third body along with the other perturbations. Söderhjelm (1975) gave a formulation of the third-body effect, but without the other effects. As applied to systems that are binary rather than triple, and where the stellar spins are (at least by hypothesis) parallel or nearly parallel to the orbit, our model does not differ from lowest order standard analyses. We confirm the following standard results:

1. On a timescale of $\sim t_{\text{TF}} I\Omega/\mu h$, the spin becomes parallel to the orbit and “pseudosynchronous,” i.e., it reaches the value at which the viscous couple W in equation (6) is close to zero (Hut 1981). The couple is an average around a Keplerian orbit, and it vanishes when the larger but short-lived couple near periastron is balanced by the weaker but longer lived (and opposed) couple at apastron. Equating W to zero gives the pseudosynchronous value of Ω_h as ω multiplied by a function of e .

2. On the longer timescale, t_{TF} , the orbit is circularized. However, both statements 1 and 2 have to be qualified by the condition that the spin angular momenta of the stars have to be suitably small when compared to the orbital angular momentum; otherwise, the binary can become either desynchronized or decircularized.

3. For triples, ignoring the effects of quadrupolar distortion, tidal friction, and GR, we obtain equations that allow the eccentricity and the mutual inclination of the inner orbit to fluctuate periodically between limits (Kozai cycles: Kozai 1962; Mazeh & Shaham 1979; KEM98). If we start with $e = 0$ and $\sin \alpha_H > (2/5)^{1/2}$ ($\alpha_H \gtrsim 39^\circ$), these cycles can have large amplitude. The maximum eccentricity reached is

$$e_{\text{max}}^2 = \frac{5}{3} \sin^2 \alpha_H - \frac{2}{3} \approx 1 - \frac{5}{3} \delta\alpha_H^2, \quad \text{if } \delta\alpha_H \equiv \frac{\pi}{2} - \alpha_H. \quad (35)$$

We see that e_{max} can approach very close to unity if α_H is only moderately close to 90° . The timescale of these cycles is of order $1/C$ (eq. [15]), and so of order P_{out}^2/P , apart from a mass-ratio-dependent factor that is only significant if the third body is much less massive than the other two.

Commonly, among observed binaries, either the orbital period is sufficiently short that tidal friction has already circularized it or sufficiently long that tidal friction is insignificant on a nuclear timescale. This is because of the high power of R_1/a in equation (7). There is only a fairly narrow range of periods, perhaps 4–5 days (but depending on mass and age), at which one might hope to find binaries in which parallelization is still taking place. However, there exists the interesting SMC radio

pulsar binary 0045 – 7319 (Kaspi et al. 1994), in which it is conjectured that, as a result of an asymmetric supernova explosion (SNEX), the NS is on an inclined orbit relative to the spin of the normal B1V component. In our first example below, we endeavor to model the process of parallelization, among others, of the B star in this system. In our second example, on the supposition that a SNEX may typically put a NS into a nonsynchronous orbit, we also consider a model of a massive star with a NS companion and various degrees of asynchronism. Such models can experience desynchronization and/or decircularization.

There is only a rather small number of known triples in which the inclination of the outer to the inner orbit is directly measured, and even fewer in which it is clearly established that this inclination is large enough to cause Kozai cycles. In fact, the system β Per (Lestrade et al. 1993) is the only example that we know. We therefore consider how the orbit of this system might have been modified at an early stage in its life, when it was a detached near-zero-age main sequence (ZAMS) system.

In binary orbits that are eccentric, but already (at least by hypothesis) parallelized and pseudosynchronized, the only part of our model that is testable is the effect of tidal distortion and GR on apsidal motion. In this respect, our model is no different from the classical model: Claret & Giménez (1993) have discussed apsidal motion, comparing observed values with those expected theoretically from the combination of quadrupole distortion and GR. For many systems, there is reasonably good agreement. For some systems, however, there is disagreement, even strong disagreement, for example, DI Her (Guinan, Marshall, & Maloney 1994) and V541 Cyg (Lacy 1998). We suspect that the discrepancies here may be due to the presence of a third body, so far undetected, although another possible reason for aberrant apsidal motion is that the stars are rotating obliquely to the orbit. The latter leads to smaller apsidal motion than expected for parallel synchronism, and the apsidal motion can even have the opposite sign (eq. [12]) if $\Omega_{1h} \lesssim \Omega_1/\sqrt{3}$. However, a third body can also contribute apsidal motion of either sign.

3.1. Parallelization, Synchronization, and Circularization in a Wide Eccentric Orbit

We consider the effect of the perturbative forces within a binary roughly based on the radio pulsar binary 0045 – 7319 in the SMC (Kaspi et al. 1994; Bell et al. 1995). In this binary (no third body is detected, or suspected), the pulsar’s orbit is quite wide ($P = 51.17$ days) and highly eccentric ($e = 0.808$). The directly measured longitude of periastron gives $\beta_J \equiv 270^\circ - \omega_{ip} = 154.76$, from equation (25). The companion B1V star appears to be unusually *inactive*: it is not a Be star and apparently has negligible wind, and the pulsar is not accreting significantly, at least not enough to be an X-ray source. These unusual circumstances (for massive NS binaries) mean that the radio orbit is unusually well defined, so that even slight changes of *orbital* parameters, due presumably to tidal friction, apsidal motion, and precession, are measurable.

We refer to the NS component as star 1, because it is descended from what was presumably the originally more massive component, and the B1V star as star 2. This choice determines which suffix belongs to which star.

Although the mass function of the pulsar is accurately known, there is only a very tentative radial velocity curve for the B star. Bell et al. (1995), assuming $M_1 = 1.4 M_\odot$, suggest the following parameters: $M_2 \sim 8.8 M_\odot$, $R_2 \sim 6.4 R_\odot$, and $L_2 \sim 1.2 \times 10^4 L_\odot$, with substantial uncertainties. The consequential inclination of the orbit to the line of sight is $\alpha_J \sim 44^\circ$ (or 136°). Bell et al. also estimate a projected rotational velocity for the B1V star of $V_{\text{rot}} \sin i \equiv R_2 |\Omega_2 \times \hat{J}| \sim 113 \text{ km s}^{-1}$, which suggests a rotational period for the star of less than 3 days, but depending on the unknown orientation of the stellar spin relative to the observer. The spin rate, although not clearly known, is marginally consistent with the possibility that the B star is in pseudosynchronism (Hut 1981). For $e \sim 0.8$, pseudosynchronism requires $\Omega_{2h} \sim 12.5\omega$ or $P \sim 4$ days. It is very likely, however, that the NS was put into its current highly eccentric orbit by a supernova “kick,” which also makes it likely that the stellar spin is inclined, perhaps quite highly inclined, to the orbit. It is, in fact, easier to account for the rate of orbital period change if the spin is retrograde, since this tends to maximize the contributions of W_2 and V_2 in equation (26).

Kaspi et al. (1996) further determined various rates of change: $\dot{P}/P \sim -2.2 \times 10^{-6} \text{ yr}^{-1}$, $\dot{\alpha}_J = 2.1 \times 10^{-4} \text{ rad yr}^{-1}$, and $\dot{\beta}_J = -4.5 \times 10^{-4} \text{ rad yr}^{-1}$. The sign of $\dot{\alpha}_J$ is different if we adopt $\alpha_J \sim 136^\circ$ instead of 44° . The accuracy of these quantities, and of $V_{\text{rot}} \sin i$, is of the order of 3%–10%.

Our model is slightly overconstrained by the current observational data, supposing that we take literally the estimate in equation (9) for the viscous timescale. We adopt the values of M_2 , R_2 , L_2 , M_1 , P , e , α_J , and β_J mentioned above. There is no evidence for a third body, and so we take $M_3 = 0$. We ignore all parameters relating to the NS except its mass, since its spin angular momentum is too small to influence the system. This only leaves the three components of Ω_2 to be assigned at $t = 0$, and there are four constraints to be satisfied: \dot{P}/P , $V_{\text{rot}} \sin i$, $\dot{\alpha}_J$, and $\dot{\beta}_J$ should all have the values listed above.

Figure 1 is a short evolutionary run starting from $\Omega/\omega = 20$, $\alpha_{\Omega_2} = 135^\circ$, and $\beta_{\Omega_2} = 0^\circ$. On such a short timescale, only β_{Ω_2} changes significantly, by precession. The plotted quantities are the ratios of the computed to observed values for the four quantities listed. It can be seen that at 195 yr, all four ratios are fairly close to unity, at which point $\beta_{\Omega_2} = 111^\circ$. We therefore adopt this as a new starting value.

Since the starting values used above were a shot in the dark, we can expect to get better agreement by some procedure such as least squares. However, the answers will be very strongly dependent on (1) the radius R_2 , which enters to the eighth power in equation (7), and (2) the estimate in equation (9) for γ , which must be very uncertain. It might be more realistic to treat γ as an unknown, in which case probably an exact solution (and possibly several, because of the nonlinearity of the equations) can be found, but it will still be very dependent on R_2 , which cannot be accurately known. Thus, we feel it is premature to attempt a definitive solution, but we feel encouraged by the fact that the model is not obviously wrong.

The evolution of the eccentricity, the component of spin parallel to the orbit (relative to the total spin), and the orbital period (relative to initial period) is shown in Figure 2a, for a timespan of about 3 Myr into the future. We started with the parameters listed above (but with $\beta_{\Omega_2} = 111^\circ$). The evolution of the B star in this interval has not been allowed for: the main sequence lifetime of an $8.8 M_\odot$ star is expected to be about 33 Myr. The perpendicular spin goes through zero at about 0.5 Myr, and the spin is almost completely parallel by 1.7 Myr. Circularization takes a good deal longer and is only half complete

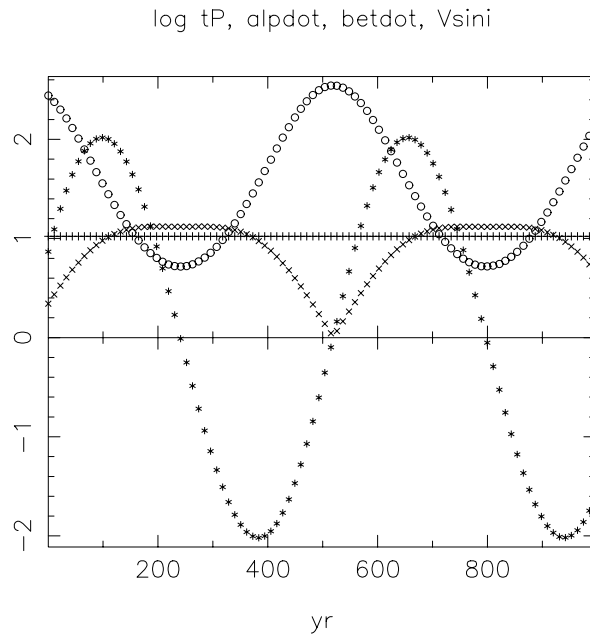


FIG. 1.—Evolution of $\log(P/|\dot{P}|)$ (*plus signs*), $\dot{\alpha}_J$ (*asterisks*), $\dot{\beta}_J$ (*circles*), and $V_{\text{rot}} \sin i$ (*crosses*) with time in a binary such as the SMC radio pulsar 0045–7319. Each quantity is divided by the observational value listed in the text. At about 195 yr, all four quantities are within about 20% of their observational values. At this point, $\beta_{\Omega_2} = 111^\circ$, having started with an arbitrary value of 0° . Such quantities as P , e , Ω , and α_{Ω_2} have not changed significantly in this short time.

by 3 Myr, but it will start to be strongly accelerated by the neglected evolutionary expansion, at this stage. Currently, $\dot{e}/e \sim -2.5 \times 10^{-7} \text{ yr}^{-1}$, on our model. This is comfortably below the upper limit found by Kaspi et al. (1996) of $7 \times 10^{-6} \text{ yr}^{-1}$.

Figure 2*b* shows the two components of spin in the orbital plane, $\Omega_2 \cdot \hat{e}$ and $\Omega_2 \cdot \hat{q}$, plotted against each other. To make the figure clearer, the viscous evolution was speeded up by a factor of $10^{8/3}$; this makes for a much less tight spiral pattern. Evolution starts slightly left of center at the top edge. The rotation axis precesses counterclockwise about 1.25 times, until the vertical component of Ω_2 ($\Omega_2 \cdot \hat{h}$, Fig. 2*a*) changes sign, and then precesses clockwise, while the two horizontal spin components diminish toward zero. Had we kept to the more realistic viscous timescale of Figure 2*a*, there would have been about 550 revolutions of the axis before it reversed direction.

Figure 2*c* shows the evolution of four timescales, also using the speeded up model of Figure 2*b*. The timescales are all given as logs, and in years. The timescale for period change $|P/\dot{P}|$ (*plus signs*) starts at $\sim 10^{3.1}$ yr, which would be roughly the required value of $\sim 5 \times 10^5$ yr if we did not speed up the viscous evolution by $10^{8/3}$. The eccentricity timescale $|e/\dot{e}|$ (*asterisks*) is about 6 times longer to start with, but is more nearly constant. The two other timescales shown are both related to apsidal motion: $1/Z$ (*circles*), and $1/|\dot{\beta}_J|$ (eq. [27]; *crosses*). The term $\dot{\beta}_J$ is the actual apsidal motion, which, however, is influenced by the precessional terms X and Y as well as by the usual apsidal motion term, Z . Prior to about 1000 yr, when the vertical spin passes through zero in the speeded-up model, the line of apses turns at a highly variable rate; probably the axis was librating rather than circulating just before this. Once the B star is no longer counterrotating, the line of apses circulates more uniformly, but with an oscillating component that diminishes as the spin becomes more parallelized.

Figure 2*d* shows two more timescales (also logged): the precessional timescale $1/(X^2 + Y^2)^{1/2}$ (*plus signs*) and the timescale of the change of inclination of the orbit to the line of sight $1/|\dot{\alpha}_J|$ (*asterisks*). The precessional rate goes through zero once, causing the cusp at ~ 1000 yr. The orbital direction oscillates about zero, causing many cusps in the log modulus of its derivative.

The origin of the present system presents some puzzles and has been the subject of recent controversy (van den Heuvel & van Paradijs 1997; Iben & Tutukov 1998; hereafter HP97, IT98). HP97 favor a history that involved Roche lobe overflow (RLOF) followed by a SNEX with an asymmetric kick, and IT98 a history that involved a common-envelope (CE) phase followed by a SNEX without a kick. We believe that neither history is satisfactory and propose a scenario that is somewhat similar to IT98 in its earlier phase (but requiring a less massive progenitor to the NS) and rather like HP97 in its later phase, requiring a SNEX kick.

We would normally expect that the system, having started with two massive main sequence (MS) stars, would have evolved through RLOF, so that star 1 (the *originally* more massive component) would have become a helium star, perhaps with a modest H-rich envelope, before heading on to C-burning, and so fairly quickly to a SNEX (HP97). However, two things argue against this:

1. If star 1 was originally over $\sim 10 M_\odot$, enough to leave a post-RLOF remnant capable of a SNEX, then RLOF should have made star 2 considerably more massive than it is now (even though its mass is by no means certain). In such RLOF, we normally expect star 2 to become more massive than the *original* mass of star 1.

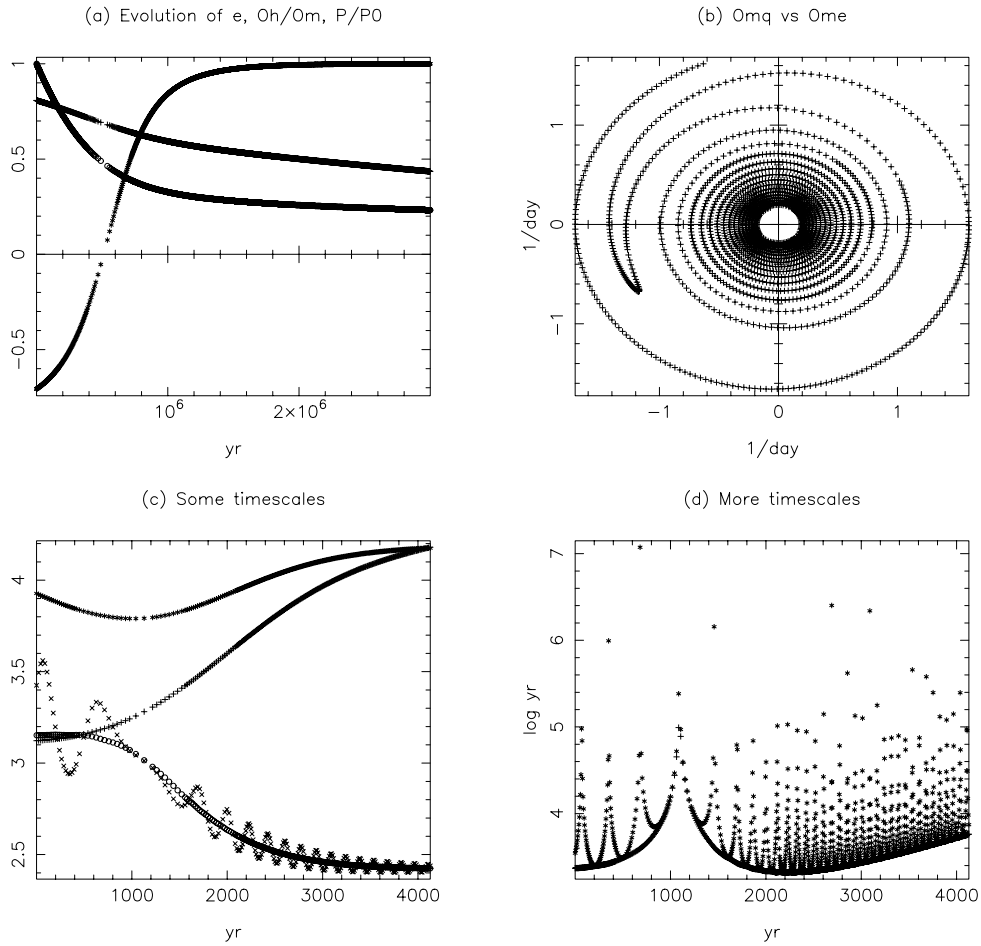


FIG. 2.—Evolution of orbit and spin in a binary such as the SMC radio pulsar 0045–7319. (a) Eccentricity (*plus signs*), cosine of the inclination of the stellar spin vector Ω_2 to the instantaneous orbital plane vector \mathbf{h} (*asterisks*), and period relative to the initial period (*circles*). The B star was started with spin inclined at $\alpha_{\Omega_2} = 135^\circ$ to the orbit ($\cos \alpha_{\Omega_2} = -0.71$), reached inclination 90° after $\sim 5 \times 10^5$ yr, and was almost completely parallelized by $\sim 1.7 \times 10^6$ yr. (b) Two components of B-star spin in the orbital plane, plotted against each other. The spin axis started at the top, left of center, turned through ~ 1.25 rotations counterclockwise, and then (at the time when the spin was exactly perpendicular to the orbit) reversed its motion to clockwise while spiralling in toward the center. The evolution was speeded up by artificially decreasing the viscous timescale by a factor of ~ 500 , to prevent the spiral being very tightly wound. The “real” timescale would have required about 600 turns before reversal. (c) Timescales $e/|\dot{e}|$ (*asterisks*) and $P/|\dot{P}|$ (*plus signs*); also the timescales $1/Z$ (*circles*) and $1/|\beta_J|$ (*crosses*) of apsidal motion (all logged). The first two timescales are artificially shortened by ~ 500 , as in (b). The last two timescales tend toward equality as the spin becomes parallelized, but precession due to nonparallel spin causes one to oscillate about the other. (d) Precessional timescales $1/(X^2 + Y^2)^{1/2}$ (*plus signs*) and the timescale $1/|\dot{\alpha}_i|$ (*asterisks*) of rate of change of inclination to the line of sight (both logged). The many cusps in the latter are due to the fact that the inclination was oscillating between two values.

2. We would expect that as a second result of the RLOF, star 2 would be a very rapid rotator, a Be star more or less, instead of the rather slowly rotating and unusually inactive star observed.

A possible answer to both these points is that

1. The initial star 1 was only moderately more massive than star 2 is now, being $\sim 12 M_\odot$.
2. The initial star 2 was little different from the star 2 now seen (the B1 star).
3. The binary was fairly wide, initially, about $P \gtrsim 50$ days.
4. Star 1 evolved to a point where its outer layers, helped by the disturbing effect of the binary companion, became unstable and blew away, first as a P Cyg star and then as a Wolf-Rayet (WR) star, perhaps without star 1 ever reaching a radius as large as its Roche lobe radius.

If star 1 did reach RLOF, this might have been more like a CE event, with much of the envelope disappearing to infinity rather rapidly and with only moderate, or perhaps even negligible, orbital shrinkage. However, we would rather categorize the process as “binary-enhanced stellar wind” (BESW), which may have altogether prevented star 1 from ever reaching its Roche lobe.

The WR binary γ^2 Vel, with $P = 78.5$ days and $e = 0.33$ (Schmutz et al. 1997), might be of the same character as the possible immediate precursor to the 0045–7319 binary, since the high eccentricity argues against there having been an episode of Roche lobe overflow. The star 2 of γ^2 Vel is an O8 III star of $20\text{--}30 M_\odot$, substantially more massive than we require. Consequently, star 1 would also have been substantially more massive originally, perhaps by about the same factor.

IT98’s model was somewhat similar to ours, except that they argued for a more massive initial star 1, $\sim 28 M_\odot$. This was required because of their desire to produce the configuration of 0045–7319 *without* an SN kick. They argued for a CE event

that reduced the period from an initial value of 27–76 days to a value of ~ 3.2 days. They postulated that the obliquity of the spin to the orbit, strongly suggested by the measured $\dot{\alpha}_J$ of Kaspi et al. (1996), is simply left over from a primordial obliquity and survived any possible tidal friction during the helium-star phase, when in their model, the orbital period was 3.2 days. A difficulty with this is that with star 1 initially so much more massive than star 2, star 2 should be rather little evolved, and should be substantially smaller than the value of $6.4 R_\odot$ suggested by Bell et al. (1995). Our model supposes a much less massive star 1, and so allows star 2 to be more substantially evolved. Our model does not predict, nor need to predict, the orbital period during the helium-burning phase; we accept the probability of an asymmetric kick, which could in principle lead to the present period if the intermediate period was anywhere in the range of ~ 3 –50 days.

Our model of the current orbital evolution might give an upper limit to the age of the system (since the SNEX) by integrating backward from present conditions. This is not a very safe process, numerically, in a dissipative system, but we made an estimate of the accuracy by integrating forward again. It appears that, in fact, the evolution *decelerates* going backward, as is hinted at by the behavior of Ω_{2h}/Ω_2 in Figure 2a. We integrated back $\sim 9 \times 10^5$ yr, reaching $P = 200$ days, $e = 0.922$, and $\alpha_{\Omega_2} = 149^\circ$; on integrating forward again, we recovered P , e , α_{Ω_2} , and Ω_2/ω to five significant figures, while β_{Ω_2} was in error by about $\sim 80^\circ$ after several thousand rotations of the Ω_2 axis. The spin period $\sim 9 \times 10^5$ yr ago is predicted to have been 1.6 days. Although it is marginal, this may be consistent with the B1V component's still being reasonably inactive, so that the model is still applicable. Thus, it is possible that the system may be as much as $\sim 10^6$ yr old in its present form. The required orbit so long ago might seem improbably long and eccentric, but one might reasonably think the present orbit improbably long and eccentric if it had been hypothesized rather than measured.

The equilibrium-tide model of tidal friction has often been considered inadequate for systems such as 0045–7319. There appear to be two main reasons, one of which we largely accept and the other which we reject. In order, they are

1. Near-equilibrium is not very likely to be established in a highly eccentric orbit; it is more reasonable in a nearly circular orbit (such as the Earth-Moon system).
2. Although turbulent convection may be a good source of friction in stars with deep convective envelopes, massive stars are only convective in their cores, where the amplitude of the tide is considered to be too small to be significant. Radiative damping in the outer layers might contribute, but this is orders of magnitude smaller.

We believe that item 2 is largely based on a highly inexact estimate of the equilibrium-tide velocity field.

If the principle is accepted that surfaces of constant density (and pressure) are always closely equal to equipotential surfaces (the basic assumption of the equilibrium-tide model), then presumably the velocity field is determinate and comes basically from conservation. Alexander (1973) and Zahn (1977, 1978) made crude estimates based on the motion being assumed either incompressible or irrotational and concluded that the amplitude of the tide (whose square is proportional to the rate of dissipation) goes to zero like r^4 , approaching the center. If the convective core were about one third of the stellar radius, then the dissipation would be down by $\sim 10^{-4}$ relative to a star with a largely convective envelope. However, EKH98 determined (their eqs. [100] to [112]) an expression for the tidal velocity field and its rate of viscous dissipation that is *exact*, to the extent that (1) the equilibrium-tide model is exact, and (2) dissipation is primarily by the effective viscosity of turbulent eddies. The velocity field is neither irrotational nor incompressible, nor does it diminish to zero like r^4 . Rather, the tidal amplitude diminishes from its surface value by less than a factor of 10 for typical MS models. Thus, the effect of dissipation in the convective core is by no means negligible: it may be down by $\sim 10^{-2}$ only. This is the basis for our estimate of γ in equation (9). In the Appendix, we briefly summarize the analysis of EKH98 regarding the factor γ .

Witte & Savonije (1999) computed the spectrum and damping rates of normal modes that can be expected to be excited in a $10 M_\odot$ star as a result of perturbation by a NS companion with the orbital parameters of 0045–7319. They obtained a braking timescale that was usually in the range of $10^{5.5}$ – $10^{6.5}$ yr. The timescale changes rapidly by factors of ~ 10 , both up and down, on timescales of only 10^4 yr or less. There are occasional excursions to values of the braking timescale as low as 10^3 yr, which result from modes resonating with harmonics of the orbital frequency. There are also occasional episodes of orbital spin-up, rather than spin-down. Such a detailed model may well be demanded by the physics, but inevitably means that the interior structure of the star will have to be very precisely known: a good deal more precise than information that is currently available. We hope that our estimate, equation (7), can serve as a crude average over a range of time of more detailed values that can only be computed if the structure and rotation of the star are known to considerable accuracy.

3.2. The Darwin and Eccentricity Instabilities

Inherent in equations (1)–(4) are at least two kinds of instability. First, there is the Darwin instability. Consider the case of a binary (i.e., no third body) in which the spin of one massive component (star 2) is parallel to the orbit and the companion (star 1) is a point-mass NS, as in the previous example. Equation (25) for $\dot{\omega}$ can be united with equation (4) for $\dot{\Omega}_2$ to give

$$t_{\text{TF2}} \frac{d}{dt} \log \frac{\Omega_2}{\omega} = \frac{\mu h}{I_2 \Omega_2} W_2 - \left(W_2 + \frac{e^2 V_2}{1 - e^2} \right) = \left[\frac{\mu h}{I_2 \Omega_2} f_a(e) - 3f_b(e) \right] - \frac{\Omega_2}{\omega} \left[\frac{\mu h}{I_2 \Omega_2} f_c(e) - 3f_d(e) \right], \quad (36)$$

where the functions f_a, \dots, f_d are all functions of e that can be evaluated from equations (5) and (6). All these functions tend to unity as $e \rightarrow 0$. It can be seen that as long as

$$\frac{\mu h}{I_2 \Omega_2} > \frac{3f_a(e)}{f_c(e)} \sim 3, \quad \text{if } e \sim 0, \quad (37)$$

then $\Omega_2 \rightarrow \omega$ as time increases. However, if the inequality in equation (37) is violated, Ω_2/ω will diverge as time increases. For a value of e that is not small, there still is a critical condition, but it is e -dependent. This well-known instability requires that the spin angular momentum $I_2 \Omega_2$ must be greater than a third of the orbital angular momentum μh (for $e = 0$).

The eccentricity instability is seen in equations (18) and (5). Specializing once again to the situation in which one star is a point mass and $e = 0$, we see that if

$$\Omega_{2h} > \frac{18}{11} \omega, \quad (38)$$

then the eccentricity starts growing exponentially. If $e > 0$ to start with, there is still the possibility of e growing, although the criterion is now e -dependent. In other words, if the star is rotating fast enough, it gives up its angular momentum in spurts sufficiently concentrated toward periastron that the companion star is flung into a wider and wider orbit, but with periastron not much changed because that is where the largely tangential impulse peaks.

Although both instabilities give exponential growth, the result can sometimes be surprisingly self-limiting. Figure 3a shows the evolution of a system whose initial configuration was unstable to both processes. We took a very massive star ($40 M_{\odot}$) evolved substantially across the MS (to $20 R_{\odot}$), put it in a 6 day, $e = 0.1$ orbit with a NS of $1.4 M_{\odot}$, and started it in parallel rotation at twice the orbital rate. We used the default values from equation (8) of the moment of inertia and quadrupolar distortion. Both the eccentricity and the degree of noncorotation (measured by Ω/ω) began to grow. For stars of comparable mass, it is difficult to violate the criterion in equation (37), but if one star is much more massive than the other, it can also be large enough, without quite filling its Roche lobe, to be Darwin-unstable (D-unstable). However, although the star spins up relative to the orbit, the orbit gains angular momentum, and so loses angular velocity, fast enough for the D-stable criterion in equation (37) to become satisfied later. After between 10^6 and 10^7 yr, the orbit first becomes D-stable and later eccentricity-stable (E-stable), and tends to both synchronism and circularity with a period of ~ 30 days. However, as before, we have ignored nuclear evolution in the massive component, which would no doubt fill its Roche lobe in little more than 10^6 yr.

Figure 3b is the same system, except that the stellar spin rate was started at 70% of corotation, rather than twice. This is substantially E-stable and very slightly D-stable to start with, but as e decreases toward zero and Ω/ω increases (although only very slightly) toward unity, at about 5000 yr the system crosses the D-unstable margin. Although both Ω and ω are going up, trying to approach synchronism, and $I\Omega$ is obviously going up, μh goes down because the orbit shrinks. Hence, the D-stable criterion in equation (37) crosses into instability, and the system begins to move rapidly away from corotation. The orbit continues to circularize, but desynchronizes and shrinks rapidly toward a collision at $\sim 19,000$ yr.

3.3. Kozai Cycles with Tidal Friction.

We now consider a problem that has a third body as well as quadrupole distortion and tidal friction. When the outer binary is sufficiently inclined to the inner binary, it is possible for the eccentricity of the inner binary to fluctuate slowly by a large amount (Kozai cycles). The amplitude of the eccentricity fluctuation depends only on the inclination, and not on the outer period or eccentricity, or third-body mass; the period of the fluctuation is of the order of $2\pi(1 - e^2)^{1/2}/C$ (eq. [15]). Even if the inner binary, when it is nearly circular, is too wide for tidal friction to play a role, the increase in eccentricity may make tidal friction important at some point in the Kozai cycle. Recall that a , like ω and P , is unaffected by the third body at our level of approximation, as shown by equation (27), so that as e increases, the periastron separation decreases. We illustrate this with the well-known semidetached binary Algol (β Per), which has a third body ($\sim 1.7 M_{\odot}$) in a 679 day orbit inclined at 100° to the semidetached pair's orbit (Lestrade et al. 1993).

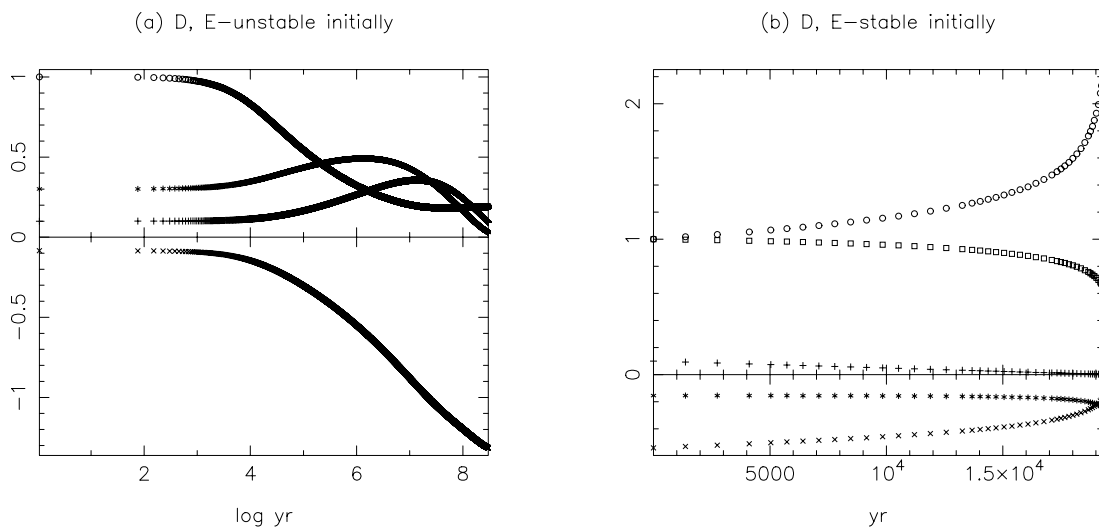


FIG. 3.—Darwin (D) and eccentricity (E) instabilities. Eccentricity (*plus signs*), orbital frequency ω relative to its initial value (*circles*), the degree of asynchronism, $\log(\Omega/\omega)$ (*asterisks*), and the ratio of spin to orbital angular momentum, $\log(I\Omega/\mu h)$ (*crosses*). Star 1 is a NS, and star 2 a massive, partly evolved MS star. The orbit has $P = 6$ days and $e = 0.1$ to start with. (a) Initially $\Omega/\omega = 2$. (b) Initially $\Omega/\omega = 0.7$. In (a), the system starts both D-unstable and E-unstable. Eccentricity and asynchronism grow, but the periastron separation remains large enough to avoid collision. Once the orbit has widened, it becomes stable to both processes and settles down. However, nuclear evolution (neglected) would cause problems before 10^7 yr. In (b), the orbit is E-stable and slightly D-stable to start with. However, as the orbit and star gradually spin up, the orbit's angular momentum goes down, while the star's goes up, leading to D-instability in about 5000 yr. After that, asynchronism increases, and the stars collide in about 19,000 yr.

In its present configuration, the inner pair is *not* subject to Kozai cycles, because the perturbation due to the quadrupole distortion of the lobe-filling component is much larger than the perturbation due to the third body. However, at an early stage in its life, β Per must have been a detached binary of two near-ZAMS stars, with radii, and therefore quadrupole moments, substantially smaller than at present.

If we believe that β Per has evolved without mass loss (ML) or angular momentum loss (AML), i.e., conservatively, we would be able to infer the period at any mass ratio, from

$$P \propto \frac{(1+q)^6}{q^3}, \quad q \equiv \frac{M_1}{M_2}. \quad (39)$$

Taking an illustrative $q_0 = 1.25$, the present period $P = 2.87$ days and $q = 0.216$ imply that $P_0 \sim 0.6$ days. However, although we accept provisionally that ML may have been negligible, there is direct and indirect evidence that cool Algols experience AML, presumably by magnetic braking in a stellar wind (Refsdal, Roth, & Weigert 1974; Eggleton 2000). For given masses, the period goes like h^3 , and so if the system lost 50% of its angular momentum, it must have started with $P_0 \sim 4.8$ days.

What we show in this subsection is that the initial period, had it been longer than ~ 3 days, would have shrunk by a combination of Kozai cycles and tidal friction to a value under 3 days in a fairly short interval of time ($\lesssim 10^7$ yr). Consequently, we have an upper limit to the amount of AML that could have taken place subsequently, once star 1 became a cool subgiant subject to magnetic braking (Eggleton 2001): about 40% of the initial angular momentum.

Figure 4 shows the evolution of a “proto-Algol” system with an initial period of 5 days: in Figure 4a, the short term; Figure 4b, the medium term; and Figure 4c, the long term. The initial Kozai cycles reach up to $e = 0.67$ (starting somewhat arbitrarily at $e = 0.1$). This value is well short of the maximum that would be reached ($e = 0.985$) if quadrupolar distortion were negligible, but is nevertheless quite large. Tidal friction near periastron at the peak of the Kozai cycles reduces the range of variation of e , although somewhat unexpectedly, by increasing the minimum eccentricity even more than by reducing the maximum. By about 10^6 yr, the eccentricity fluctuates between 0.47 and 0.53, and both the range and the mean reduce until, by 10^7 yr, the orbit is circularized at $P \sim 2.1$ days.

A point to note is that the inclination α_H of the inner orbit to the outer orbit changes somewhat during the process. We started from 97.5° in order to end up with the currently observed value of 100° . For longer initial periods, the change is larger, which probably means that the period was not in practice much longer than ~ 10 days before the Kozai cycling and tidal friction reduced the period to ~ 2 days.

It is not clear how triple systems, and especially such close triple systems, formed in the first place, but a possible mechanism, arguably the least unlikely, is that fairly early on in the star-forming process, when the stellar density was higher than it is now, two primordial binaries had a near collision, with one component of one binary captured by the other binary, and the other component ejected. In this scenario, angles near 90° are much *more* likely than those near 0° .

Table 1 shows how the period P_{end} at the end of the shrinkage process depends on the period P_0 at the beginning, for our specific proto-Algol system. It also shows the time taken in the shrinkage and circularization process, which is always small compared to the expected nuclear lifetime of the system (~ 1 Gyr), and gives the starting value of mutual orbital inclination α_H that ends up as the current value of 100° . Assuming that this inclination is distributed randomly, in a capture process, the range 80° – 100° has probability $\sim 17\%$, and the range 86° – 94° about 7% .

The combination of Kozai cycles plus tidal friction should mean that there is a shortage of triple systems with (1) fairly high inclination of one orbit to the other and (2) inner periods above perhaps 3–4 days. This will be difficult to confirm, since it is

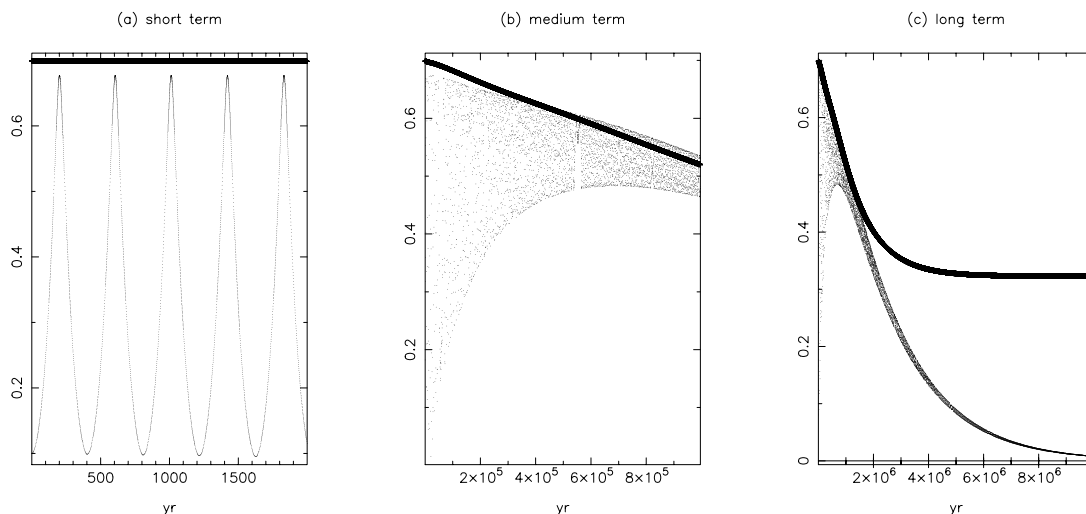


FIG. 4.—Evolution of eccentricity (dots) and $\log P$ (thick line) in the inner binary of a proto-Algol triple system. The initial orbital parameters are $[(2.5 + 2 M_\odot; 5 \text{ days}, e = 0.1) + 1.7 M_\odot; 679 \text{ days}, e = 0.23; \alpha_H = 97.5^\circ]$. (a) First 2000 yr, showing somewhat truncated Kozai cycles; (b) First 10^6 yr, showing the orbit settling toward a nearly constant, but slowly decreasing, eccentricity; (c) First 10^7 yr. By 10^7 yr, $e \sim 0$, $P \sim 2.1$ days, and $\alpha_H = 100^\circ$. Some apparent structure in the eccentricity variation in (b) is due to beating between the data-plotting frequency and Kozai-cycle frequency, which can be commensurable.

TABLE 1
PROTO-ALGOL BINARIES WITH DIFFERENT
INITIAL PERIODS

P_0 (days)	P_{end} (days)	T_{circ} (yr)	i_0 (deg)
3.....	2.8	3×10^7	99.8
5.....	1.9	1×10^7	97.3
10.....	1.7	8×10^5	95.0
15.....	0.8	9×10^4	94.0

very difficult to determine the inclination of one orbit to another. SS Lac (below) is a triple in which we infer $\alpha_H \sim 29^\circ$, which is not enough to give significant Kozai cycling; thus, the inner period of 14 days does not conflict with our conclusion. If inclinations are indeed distributed at random, then $\sim 50\%$ of triples have $60^\circ \lesssim \alpha_J \lesssim 120^\circ$, and a quite substantial deficit of systems with inner periods longer than about 3–4 days can be expected.

4. AN APPLICATION TO SS LAC

SS Lac is a binary that eclipsed before about 1950, but not subsequently. A likely explanation was the presence of a third body in a noncoplanar orbit, and this was confirmed by TS00, who found long-period orbital motion in the CG of the short-period pair. By coincidence, the longer period in SS Lac is exactly the same as that in Algol (679 days). Following TS00, we refer to the three components as Aa (star 1), Ab (star 2), and B (star 3), and the two binaries as A and AB. TS00 also reanalyzed historic light curves of the period 1890–1930, obtaining a mean light curve assigned to epoch 1912. Their spectroscopic data refer to epoch 1998. In this section we model the dynamical evolution over the period 1912–1998, trying to find a model that gives the end of eclipses in 1950.

In general, our model requires 25 input parameters, which we list here in two groups:

$$Q_{Aa}, I_{Aa}, \Omega_{Aa}, L_{Aa}, \quad Q_{Ab}, I_{Ab}, \Omega_{Ab}, L_{Ab}; \quad (40)$$

$$M_{Aa}, R_{Aa}, M_{Ab}, R_{Ab}, \quad P_A, e_A, \quad M_B, P_{AB}, e_{AB}, \quad \alpha_H, \beta_H, \alpha_J, \beta_J. \quad (41)$$

However, the A binary is sufficiently wide ($P \sim 14$ days) that, provided that its eccentricity (or more specifically, its perihelion separation) does not vary by a substantial factor, except perhaps intermittently, tidal friction should be quite unimportant. More helpfully still, the Q -dependent distortion terms that determine X , Y , and Z in equations (1)–(4) are unimportant compared to the third-body terms (components of the tensor S) in these equations, so that all of the quantities listed in equation (40) are negligible. The radii R_i and the angles α_J and β_J defining the direction to the observer are also unimportant for the orbital evolution, although they matter for the eclipses and the date of their cessation. Although the Q_i have little influence on the orbit, they do have a marked effect on the spins of the stars because of the couple they cause, as we mention briefly below.

This reduces our significant input file to the 13 quantities listed in equation (41). Of these, e_A , P_A , e_{AB} , and P_{AB} are well or very well determined at epoch 1998 (TS00). Although e_A may have (indeed will have) changed since epoch 1912, the other three quantities can be supposed constant. This is because, in our model:

1. At the level of the quadrupole approximation for the perturbing force of the third body, the AB orbit is exactly constant.
2. The perturbing force on the A orbit in the absence of tidal friction is a potential force, and hence does not supply energy to the A orbit when integrated over an approximately Keplerian orbit; this means that the semimajor axis a_A and the period P_A are constant, even though e_A and h_A are not.

Thus, among these four quantities, only e_A (1912) must be guessed and ultimately solved for on the basis that in 86 yr, the 1998 value (0.136) must be reached (in conjunction with other constraints).

Similarly, the three masses are constrained, but not uniquely determined, by three observed-mass functions at epoch 1998. We need the two 1998 inclinations, i_{AB} and i_A . TS00 estimated the latter on the basis that (i) $i_A(1912) = 87^\circ.6$ is known from the eclipse analysis, (ii) those data implied that i_A must have been $81^\circ.6$ in 1950, when eclipses ceased, and (iii) i_A has been decreasing at a constant rate since 1912. We find that in general, the rate of change of i_A is not very constant, and so we make a guess at the 1998 value of i_A , which, of course, has to be consistent with the value that emerges from the calculation. The starting value α_J is just $\alpha_J \equiv i_A(1912) = 87^\circ.6$.

We also have to know or guess i_{AB} . This, however, is constant in time, since \hat{H} (see point 1 above) and \hat{J} are constant vectors in space, even though their components in the e, q, h frame vary as the frame itself rotates. Dotting the vector $\hat{H} = (\sin \alpha_H \cos \beta_H, \sin \alpha_H \sin \beta_H, \cos \alpha_H)$ into the vector $\hat{J} = (\sin \alpha_J \cos \beta_J, \sin \alpha_J \sin \beta_J, \cos \alpha_J)$, we have

$$\cos i_{AB} = \cos \alpha_H \cos \alpha_J + \sin \alpha_H \sin \alpha_J \cos (\beta_H - \beta_J). \quad (42)$$

We therefore have to know or guess α_H and $\beta_H - \beta_J$ in 1912, α_J being known.

TS00's analysis of the ~ 1912 light curve gave an inclination of $87^\circ.6$, as mentioned above. They also obtained the longitude of periastron ω_{1p} , related to β_J by equation (18). The β_J from TS00's 1912 light curve is $121^\circ.6$ (see their Table 6, giving ω_{1p} , and differing slightly from their Table 5 value for reasons that they explain). However, this value is based on the assumption that e_A is constant, and we find that generally it is not. The most significant orbital quantity that is given by the light-curve analysis, as TS00 explain, is the departure $\Delta\Phi_{E2} = -0.072$ of eclipse 2 from phase 0.5 relative to eclipse 1. For moderate

eccentricities,

$$\frac{\pi}{2} \Delta\Phi_{E2} \approx e_A \cos \omega_{1p} \equiv -e_A \sin \beta_J = -0.1128 . \tag{43}$$

For $e_A = 0.136$, this gives the value of β_J mentioned above. However, in our best near-solutions, we usually find e_A increasing, i.e., it started in 1912 with a smaller value. Evidently, it cannot have been smaller than 0.1128. Our preferred starting value is 0.115, and this implies $\beta_J = 101^\circ.2$. A value above rather than below 90° is preferred, because TS00's value of $e_A \sin \omega_{1p} = -e_A \cos \beta_J$, although substantially less well determined, is fairly definitely positive.

It may seem rather unsatisfactory that our preferred $e_A(1912) = 0.115$ is very close to the minimum value 0.1128 inferred from eclipses. However, what can be seen as “special” about the system is rather the fact that the 1998 value of β_J is extremely close to 90° : $91^\circ.7 \pm 0^\circ.6$ (TS00, their Table 2, giving $\omega_{1p} = 178^\circ.3$). Such a value, viewing the system almost exactly along the latus rectum, favors the maximum departure ($\Delta\Phi_{E2}$) of the secondary eclipse from phase 0.5. If we imagine, going backward in time, that e_A does *not* change, then we are driven to postulate a rather large change in β_J to the TS00 value $121^\circ.6$, to allow for the fact that the eclipses were substantially closer than this maximum value in 1912. What we conclude here is that less apsidal motion was necessary, because the eccentricity was a little smaller in 1912. We would quite generally expect that eccentricity changes on the same timescale as apsidal motion. Both timescales are dictated primarily by the coefficient C in equation (15), if, as for SS Lac, only the third-body perturbation is significant.

Our guess at the initial value of e_A therefore provides us, from eclipse data, with a starting value for β_J via equation (43). We already have $\alpha_J \equiv i_A = 87^\circ.6$ from TS00's light curve data. We have to make two further guesses at the angles α_H and β_H that in 1912 gave the orientation of \hat{H} .

To summarize, of the 13 quantities that we need to start with in 1912, four are known directly from observation: these are P_A , P_{AB} , and e_{AB} from the 1998 radial velocity curves and $\alpha_J \equiv i_A$ from the 1912 light curve. If we then guess the following four quantities, i_A in 1998 and the three starting values e_A , α_H , and β_H in 1912, we can work out the remaining six starting values from the following six observationally determined quantities: three mass functions from the 1998 radial velocity curve and two fractional radii and the phase lag $\Delta\Phi_{E2}$ from the 1912 light curve. Having integrated the equations for the 86 yr timespan, we then have four further pieces of observational data to constrain our four guesses. Three of these are e_A and $\beta_J \equiv 270^\circ - \omega_{1p}$ in 1998 and the cessation of eclipses in 1950. We determine a theoretical T_E , the time of cessation, as the average of the two times after $t = 0$ (1912) at which the two series of eclipses (primary and secondary) stopped. The observational value to match is $T_E = 38$ yr. The fourth and last constraint on the four guesses is that the value for i_A in 1998 should equal the value guessed in the first place. Table 2 lists the values used, taken from TS00, and also lists our approximate solution.

Table 2 groups parameters under “observed,” “guessed,” and “computed.” All the observational data are taken from TS00. Our guess was based on a preliminary eyeball search of parameter space and refined by trial and error.

Since the differential equations are nonlinear, there is no guarantee either that a solution satisfying all the constraints exists, or that if it does, it is unique. However, our very brief search located one quite accurate solution with a fairly modest inclination between the orbits (29°), and a rather more extended search suggested that there were unlikely to be any other solutions, except possibly at high inclination, at which the behavior can become rather chaotic. Another possibility, which we have not explored, is that the orbital inclination has decreased from $92^\circ.4$ rather $87^\circ.6$ in 1912.

Figures 5a and 5b illustrate some aspects of the model. Figure 5a follows the orbital evolution for 1912–1998, and Figure 5b follows it for slightly over 3000 yr. The date is plotted horizontally, and the phase (from 0 to 2, so that two complete cycles are shown) vertically. In Figure 5a, eclipses occurred within the narrow cigar-shaped areas centered at 0.24 (star 1 \equiv Aa eclipsed by star 2 \equiv Ab) and 0.81 (Ab eclipsed by Aa). The one at 0.24 was slightly deeper and narrower, in 1912 (TS00). The phase in this figure is measured from periastron. Also shown, starting near 0.24 and 0.8, are the two phases of points determined by equations (32) and (34).

In Figure 5b, the same information is given for a much longer time span: 1912–5250. Small leaf-shaped patches now indicate the episodes of eclipses, and the curves indicating the two phases slope generally downward because of apsidal advance (and other rotation of the orbital frame). It can be seen that the next series of eclipses is not to be expected until about

TABLE 2
SYSTEM PARAMETERS FOR SS LAC

Parameter	Observed	Guessed	Parameter	Observed	Computed	Parameter	Observed	Computed
P_{AB} (days)	679		$\Delta\Phi_{E2}$	-0.072		R_{Aa}/a_A	0.0741	
e_{AB}	0.159		β_J (deg)		101.2	R_{Ab}/a_A	0.0715	
P_A (days)	14.416		i_{AB} (deg)		75.7	$a_A (R_\odot)$		44.7
$\alpha_J \equiv i_A$ (deg)	87.6		$f'_{Aa} (M_\odot)$	2.56		$R_{Aa} (R_\odot)$		3.36
$\alpha'_J \equiv i'_A$ (deg)		73	$f'_{Ab} (M_\odot)$	2.49		$R_{Ab} (R_\odot)$		3.20
e_A		0.115	$f'_B (M_\odot)$	0.22		e'_A	0.136	0.138
α_H (deg)		29	$M_{Aa} (M_\odot)$		2.93	β'_J (deg)	91.7	91.6
β_H (deg)		37	$M_{Ab} (M_\odot)$		2.85	T_E (yr)	38	37.7
			$M_B (M_\odot)$		0.798	α'_J (deg)		72.9

NOTE.— $f'_{Aa} = M_{Aa} \sin^3 i'_A$; $f'_{Ab} = M_{Ab} \sin^3 i'_A$; $f'_B = M_B \sin i'_{AB}/(M_{Aa} + M_{Ab} + M_B)^{2/3}$. Primed quantities refer to epoch 1998; all others, apart from T_E , refer to epoch 1912 or to constants.

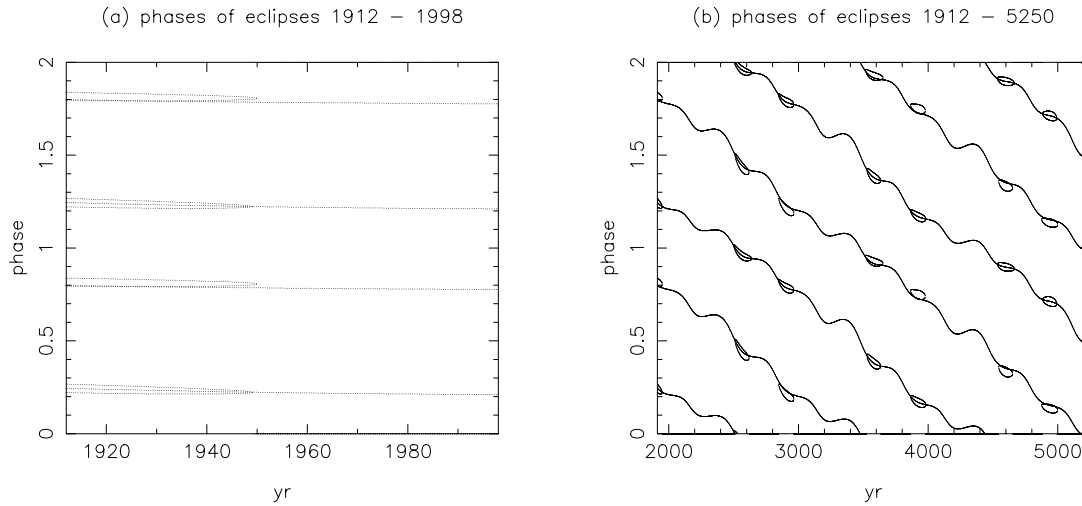


FIG. 5.—(a) Phases of eclipses of SS Lac, as computed here for 1912–1998. Two whole cycles are shown on the vertical axis. Phase zero is periastron. Eclipses occur in the narrow cigar-shaped areas centered at phases 0.24 (star 1 in front) and 0.81 (star 1 behind), and ending at about 1950. Also shown are two phases: first, starting near 0.24, the phase where star 1 crosses the plane containing the line of sight and the orbital axis, star 1 in front (eq. [32]), and second, starting near 0.8, the phase where the radial velocity of star 1 relative to the CG of the inner binary is zero and decreasing (i.e. star 1 behind; eq. [34]). The slight effect on the phase of the orbital motion of the inner binary within the outer binary has been ignored. (b) Same as (a), but for the interval 1912–5250. Regions of eclipses are now leaf-shaped. The sloping lines can be identified by comparing the left-hand edge with the whole of (a). The slopes indicate that periastron is, on the whole, advancing, but occasionally retreats because of precession.

2500. Epochs when eclipses take place appear to be separated alternately by a long interval and a shorter interval, and unfortunately we seem to be entering a long interval. Each period of eclipses lasts about a century.

The fact that the two phases decrease (mostly, but not always) relative to the phase of periastron, as seen in Figure 5b, is, of course, due to the motion of the orbital frame. If this motion were just apsidal motion, i.e., if the major axis were rotating only about the angular momentum axis, we would have a relatively simple relation between the anomalistic period (periastron to periastron) and the sidereal period (successive passages through a plane fixed in an inertial frame and containing the CG), and the two phases in Figure 5b would have a constant slope. However, with precession as well, the relation between the two periods can be rather complex. From the point of view of our simple model, it is the anomalistic period that is “basic:” if the perturbing forces, however many of them, are conservative, then the anomalistic period P as given by equation (16) is a constant at our level of approximation.

The period of precession of the inner orbit is about 1000 yr, and the inclination to the line of sight (α_j) oscillates between about 47° and 105° . The inclination of the inner orbit relative to the outer oscillates by only about 1° . It is inherent in our level of approximation that the inner angular momentum should be small compared to the outer, and unfortunately this is hardly true for SS Lac, but the fact that the inner orbit oscillates so little may nevertheless make the solution reasonably valid.

We do not discuss the accuracy of the input data and of our fit in detail, for four reasons:

1. TS00 discuss fully the accuracy of the observational data. We have used only values that are independent of their assumptions that (1) e_A is constant, and (2) $\alpha_j \equiv i_A$ and $\beta_j \equiv 270^\circ - \omega_{ip}$ change at constant rates. All the standard errors are less than 1%, except for e_{AB} (13%), $\Delta\Phi_{E2}$ (6%), f_B (3%), R/a (3%), and T_E (3%); e_{AB} only appears in C , equation (15), and in a very nonsensitive way.

2. We have zero degrees of freedom and four constraints to satisfy, with four unknowns, and so if we can find a solution at all, it will be exact, to the extent that the data are. A hypothetical problem is that there might be functional dependences among the constraints, but the fact that our eyeball search converged very rapidly suggests that there are not. Varying each of our three guessed angles by 1° usually gave a much worse fit, and so did varying e_A (1912) by 0.001. Hence, we believe that the guesses are right to about this level of accuracy.

3. By defining the computed value of T_E as the average of the two times at which the two series of eclipses disappear, we make it a discontinuous (stepwise) function of the input, and therefore cannot differentiate it smoothly. We could develop a more sophisticated definition, but this seems unnecessary in view of the rather good solution found by trial and error.

4. The main uncertainty is possible systematic error, such as the possibility that equations (1)–(4) are wrong. We had hoped to find more constraints than unknowns, and so test the theory more rigorously.

We can, however, make some predictions that are testable: for example, the inclination i_A should decrease to 70° in 2011 and to 65° in 2039. This should produce a measurable change in the mass function. The eccentricity should be currently approaching its peak of ~ 0.138 , and so may not change significantly for about 30 yr, but should drop to 0.132 by 2040. It should reach a minimum of 0.09 in 2160.

Figure 6 illustrates two possible behaviors of the spin Ω_1 . The three components in the instantaneous orbital frame are shown as functions of time. The stars were started, arbitrarily, with $\Omega = \omega$. If the stars were perfect spheres, they would simply maintain constant (vectorial) spin in an inertial frame, tidal friction being negligible in this system, and so oscillate sinusoidally in the frame of the precessing inner binary. However, because they have quadrupole moments, due partly to their spin

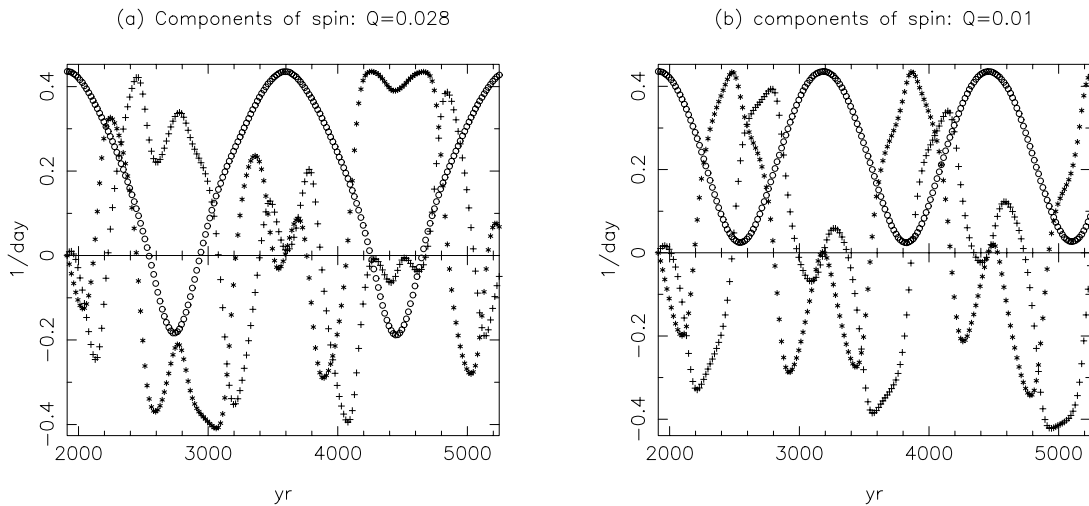


FIG. 6.—Three components of the angular velocity of star 1 in SS Lac as functions of time: Ω_{1h} (circles), Ω_{1e} (plus signs), and Ω_{1q} (asterisks). (a) $Q_1 = Q_2 = 0.028$; (b) $Q_1 = Q_2 = 0.01$. In both cases, the system was started with parallel corotation.

and partly to their gravitational effect on each other, there are couples on them. In Figure 6a, we used our default value of $Q = 0.028$ ($n = 3$ polytrope), and in Figure 6b, reduced this to 0.01. We have tried other values of Q and do not see any very simple relation between the size of Q and the amplitudes or other characteristics of the oscillations. Considering that the orbit precesses on a cone of half-angle 29° , it seems surprising that the rotation axes of the component stars (we only plot star 1 \equiv Aa) can turn by more than 90° in the course of ~ 500 yr.

It may be questioned whether the approximation that we make in this paper, that a star rotates with a unique Ω as if it were rigid, is sustainable in circumstances in which Ω is changing in direction by a large amount in a few hundred years. Tidal friction is the agency that we rely on to achieve this: provided that the structure of a star is not strongly dependent on the velocity field within it, viscous dissipation should ensure that a nonuniformly rotating star evolves toward its minimum-energy state (for a given angular momentum) of uniform rotation. Although tidal friction *between* the two components of system A in SS Lac is probably negligible, tidal friction *within* either Aa or Ab is expected to operate on the timescale t_V of equation (9), i.e., decades. Thus, it seems quite possible that the star is indeed kept fairly near a state of uniform rotation, despite major changes in the direction of its rotation axis.

V907 Sco (B9.5 V + B9.5 V; 3.78 days, $e = 0$; Lacy, Helt, & Vaz 1999) is another system in which eclipses come and go, even more dramatically than in SS Lac. It eclipsed in the intervals 1899–1918 and 1963–1986, and not in 1918–1963, or after 1986. Lacy et al. (1999) detected the third body, also from the motion of the CG of the short-period pair, with $P_{\text{out}} = 99.3$ days and $e_{\text{out}} \sim 0$. Unfortunately, an analyzable light curve for this system during its eclipsing phase does not exist, for reasons mentioned by Lacy et al. (1999), and thus we have less rather than more data with which to test our model.

5. DISCUSSION

Our formulation of the combined effect of five different perturbations on a Keplerian orbit, while very simple, appears to give physically believable results in a number of cases. It is, however, not easy to find observational data on stellar orbits that will seriously test the model. A major uncertainty is the viscous timescale of a star. One can question whether anything so simple as a unique viscous timescale can be adequate. However, the timescale estimated from first principles in the Appendix seems surprisingly reasonable for the radio pulsar system 0045–7319.

The model gives a determination of the orientation of the outer orbit in the triple system SS Lac, and although not overconstrained by data currently available, may be challenged by data that should be available in a few decades. However, in this system, the quadrupole distortions of the stars are sufficiently insignificant that only the third-body terms are being tested here.

A potentially significant statistical effect is predicted on the basis of the combination of tidal friction with Kozai cycles. We have argued that if the outer orbit in a triple is moderately highly inclined to the inner, then the inner orbit is likely to be shrunk to a limiting value of only 2 or 3 days, supposing that it “started” at a longer period. This limiting period will depend on the outer orbital period and also on the rotation rate of the stars, among other parameters. Roughly, it is dictated by the fact that for substantial Kozai cycles, we need $C \gtrsim Z$, from equations (12)–(15). This would give a longer limiting period for systems with a longer P_{out} than β Per. On some models of triple star formation, inclinations larger than 60° are as likely as not, and so we might expect a significant deficit of orbits above some value in triples, relative to those in binaries. A. A. Tokovinin (1998, private communication) has noted that in his multiple-star catalog (Tokovinin 1997), the distribution of periods among spectroscopic binaries that are in triples tends to drop off above 5 days, whereas among those that are not in triples, it continues to rise.

We have not yet been able to incorporate in the model a satisfactory approximation for what we believe is a very important further perturbation to binary orbits: the effects of ML and AML, such as is likely to be experienced by cool stars with active dynamos in their outer convection zones. If a star is subject to spherically symmetric ML, the mass lost carries off orbital

angular momentum as well as spin angular momentum: the amount of the latter may be enhanced if there is magnetic linkage between the star and the wind out to some substantial Alfvén radius. However, ML is unlikely to be very spherically symmetric. Also, some of the wind may well be accreted by the companion star, and furthermore, during the accretion process there is often found to be further mass loss (ML) and presumably angular momentum loss (AML), in the form of bipolar jets from the inner portion of the accretion disc. A variety of possible models for the ML/AML process can be thought of, but the physical process that they attempt to model may be too dependent on the details of how the gas actually travels from one star, either to the other or to infinity, to admit even at first order a simple yet credible formulation. We hope to attempt this in the future.

An example in which this may well be important is the young and active binary BY Dra (K1Ve + K1Ve; 6 days, $e = 0.5$; Vogt & Fekel 1979). One of the two components shows rotational modulation with a period of 4 days. This is too slow for pseudosynchronism, which at such high eccentricity implies a rotation period of 2 days. A possible answer is that the component is in a state of transient equilibrium between magnetic braking, which would tend to slow it down, and pseudo-synchronization, which would tend to speed it up. It is by no means improbable that these two timescales are comparable in this system.

Both the concepts of tidal distortion and of tidal friction will, we hope, be testable with some three-dimensional numerical modeling of stellar interiors that is currently being developed: the DJEHUTY project. This project aims at applying existing and well-tested three-dimensional hydrodynamic and thermodynamic (but non-self-gravitating) grid-based algorithms to the self-gravitating situation of stellar interiors, using massively parallel hardware. Although the resolution currently aimed for, of $\sim 10^8$ cells, would not be enough to resolve the surface layers of tidally distorted stars, it may well be adequate to resolve the interiors, and so determine whether dissipation in convective cores may be an effective agent of tidal friction, as we suggest here.

This work was performed under the auspices of the US Department of Energy by the University of California, Lawrence Livermore National Laboratory, under contract W-7405-Eng-48.

APPENDIX

EFFECTS OF PERTURBATIVE PROCESSES

The analysis that gives (1) the extra forces due to the five perturbative processes listed at the beginning of § 1, and (2) their effect on the orthogonal triad e , q , h is largely taken from EKH98, except for the third-body perturbation that was described in KEM98 and GR, which is well known. However, EKH98 contains a mistake of a factor of 2 in the part of the gravitational potential that is due to the distortion of the stars by their mutual gravitational interaction. We are grateful to R. Mardling (2000, private communication) for pointing this out. We list here the equations of EKH98 that have to be changed: equations (36), (38), (75), (76), and (97). In each of these, the last term on the right, i.e., the term that does *not* involve Ω , should be divided by 2. This has no effect on the overall analysis in that paper. Equation (12) of the present paper, based on equation (97) of EKH98, contains the correction.

Equations (10) and (11) of the present paper are obtained from equations (88)–(96) of EKH98. In EKH98, expressions were given for the rate of change of the Euler angles giving the orientation of the e , q , h frame relative to an inertial frame. In fact, the X , Y , and Z terms given here are what emerge more directly from the analysis; although not given explicitly in EKH98, they can be recovered from the formulae for rates of change of Euler angles given there.

The timescale t_F for tidal friction that we use in this paper has been redefined to be twice the value that was used in EKH98.

A novel result of EKH98 was a determination, exact to the order that we work to here, of the velocity field in a rotating star that, in the frame that rotates with the star, suffers a time-dependent tidal perturbation due to the presence of the other star. Time dependence can arise because the orbit is elliptical and/or not in corotation with the star. We summarize the result here.

In the equilibrium-tide model, we approximate that the density (as well as the pressure) is constant on equipotential surfaces of the instantaneous gravitational field of the companion. This means that

$$\rho = \rho(r_*), \quad r_* = r + r\alpha(r)P_2(\cos \theta), \quad (\text{A1})$$

where $\alpha(r)$ is a dimensionless function that gives the ellipticity of an equipotential as a function of distance from the center. The angle θ is measured from the direction of $d(t)$, the separation of the two stellar centers. Radau's equation

$$\alpha'' - \frac{6\alpha}{r^2} + \frac{8\pi r^3 \rho(r)}{m(r)} \left(\frac{\alpha'}{r} + \frac{\alpha}{r^2} \right) = 0, \quad (\text{A2})$$

gives $\alpha(r)$, apart from a multiplicative factor that gives $\alpha = \alpha_1$ at the surface $r = R_1$, where

$$\alpha_1 = - \frac{M_2 R_1^3}{M_1 d^3} \frac{1}{1 - Q}. \quad (\text{A3})$$

The term Q is related to the classical apsidal motion constant k_2 :

$$k_2 \equiv \frac{1}{2} \frac{Q}{1 - Q}. \quad (\text{A4})$$

Let

$$F(\mathbf{r}, \theta) \equiv r^2 P_2(\cos \theta) = \frac{3}{2} (\mathbf{k} \cdot \mathbf{r})^2 - \frac{1}{2} r^2, \quad (\text{A5})$$

where $\mathbf{k} \equiv \mathbf{d}/d$. Since \mathbf{d} is time-varying, both α and \mathbf{k} depend on t , the former because $\alpha \propto 1/d^3$ (eq. [A3]). Then, with ρ as a function of r_* only and r_* viewed as a function of \mathbf{r} and t , we obtain

$$\frac{\partial \rho}{\partial t} = \frac{d\rho}{dr_*} \frac{\partial r_*}{\partial t} = \frac{d\rho}{dr_*} \left(\frac{\partial \alpha}{\partial t} \frac{F}{r} + \frac{3\alpha G}{r} \right) = \frac{3\alpha}{r} \frac{d\rho}{dr_*} \left(-\frac{1}{d} \frac{\partial d}{\partial t} F + G \right), \quad (\text{A6})$$

where

$$G(\mathbf{r}, \theta) \equiv \frac{1}{3} \frac{\partial F}{\partial t} = \mathbf{k} \cdot \mathbf{r} \frac{\partial \mathbf{k}}{\partial t} \cdot \mathbf{r}. \quad (\text{A7})$$

The functions F and G are obviously orthogonal harmonic functions of degree 2.

Now consider the velocity field given by

$$\mathbf{v} = \frac{3\alpha_1}{2} \beta(r) \left(\frac{1}{d} \frac{\partial d}{\partial t} \nabla F - \nabla G \right). \quad (\text{A8})$$

Then

$$\nabla \cdot \rho \mathbf{v} = \frac{3\alpha_1}{r} \frac{d\rho\beta}{dr} \left(\frac{1}{d} \frac{\partial d}{\partial t} F - G \right), \quad (\text{A9})$$

and we can see that equation (A1) is satisfied to first order, provided that

$$\frac{d\rho\beta}{dr} = \frac{\alpha}{\alpha_1} \frac{d\rho}{dr}, \quad \text{i.e. } \beta = \frac{1}{\rho\alpha_1} \int_{R_1}^r \alpha \frac{d\rho}{dr} dr. \quad (\text{A10})$$

The lower limit in the integral comes from the boundary condition that the outer surface ($\rho = 0$) is a surface that moves with the fluid, so that the velocity must be finite there, despite the vanishing density. The function $\beta(r)$ is determined unambiguously by the structure of the star, via equation (A3) determining $\alpha(r)$, and is well behaved ($\beta \rightarrow 1$) for polytropic ($0 < n < 5$) surfaces as $\rho \rightarrow 0$, despite the apparent singularity there.

Using suffix notation,

$$v_i = \frac{3\alpha_1}{2} \beta(r) s_{ij} x_j, \quad \text{where } s_{ij} \equiv \frac{1}{d} \frac{\partial d}{\partial t} (3k_i k_j - \delta_{ij}) - k_i \frac{\partial k_j}{\partial t} - \frac{\partial k_i}{\partial t} k_j. \quad (\text{A11})$$

The rate-of-strain tensor is now seen to be

$$t_{ij} \equiv \frac{\partial v_i}{\partial x_j} + \frac{\partial v_j}{\partial x_i} = \frac{3\alpha_1}{2} \left[2\beta s_{ij} + \frac{\beta'}{r} (s_{ik} x_k x_j + s_{jk} x_k x_i) \right]. \quad (\text{A12})$$

We square this and average it over an equipotential (which at this level of approximation can be taken to be spherical), to obtain

$$\frac{1}{4\pi} \int t_{ij}^2 d\Omega = 9\alpha_1^2 s_{ij}^2 \left(\beta^2 + \frac{2}{3} r\beta\beta' + \frac{7}{30} r^2 \beta'^2 \right). \quad (\text{A13})$$

Now,

$$s_{ij}^2 = 6 \left(\frac{1}{d} \frac{\partial d}{\partial t} \right)^2 + 2 \left(\frac{\partial \mathbf{k}}{\partial t} \right)^2 = \frac{2}{d^2} \left[2 \left(\frac{\partial d}{\partial t} \right)^2 + \left(\frac{\partial \mathbf{d}}{\partial t} \right)^2 \right], \quad (\text{A14})$$

and so the rate of dissipation of mechanical energy is

$$\begin{aligned} \dot{E} &= -\frac{1}{2} \int \rho w l t_{ij}^2 dV \\ &= -\frac{9\alpha_1^2}{d^2} \left[2 \left(\frac{\partial d}{\partial t} \right)^2 + \left(\frac{\partial \mathbf{d}}{\partial t} \right)^2 \right] \int_0^{M_1} w l \left(\beta^2 + \frac{2}{3} r\beta\beta' + \frac{7}{30} r^2 \beta'^2 \right) dm. \end{aligned} \quad (\text{A15})$$

The parameters $w(r)$ and $l(r)$ are the mean velocity and mean free path of turbulent eddies. The β -dependent weight factor in parentheses in equation (A15) is what we call $\gamma(r)$, and its average over the turbulent convective region of the star is the γ_1 of equation (9). The factor in square brackets in equation (A15) leads to a functional form of the tidal friction force, since it depends on the (variable) separation d , which is the same as the result usually obtained by arguing that the tidal bulge lags the line-of-centers by some small fixed amount. Averaged over a Keplerian orbit, it gives V and W (eqs. [5] and [6]), and those parts of the terms X , Y , and Z in equations (10)–(12) that arise from tidal friction. The details are given in EKH98.

Although a common approximation for $\alpha(r)$ is $\alpha \propto r^3$, and it is commonly argued from this that, in effect, $\beta \propto r^4$ and $\gamma \propto r^8$, none of these approximations is at all reliable. EKH98 integrated two polytropic models and two MS stellar models. In the $n = 3$ polytrope, it was found (EKH98, Fig. 1) that α and β decrease by a factor of about 10, from the surface right to the center. At the surface, β is unity, and γ therefore somewhat larger (~ 4). In the central one-third by radius, roughly the region of convection in an upper MS star, $0.01 \lesssim \gamma \lesssim 0.03$. We therefore feel that an estimate of a mean $\gamma \sim 0.01$ is reasonable for MS stars that are typically slightly more centrally condensed than an $n = 3$ polytrope.

The approximation $\alpha \propto r^3$ is appropriate to the outer layers of a star, in which the density is low compared to the mean density: in this case, equation (A2) gives $m' = 0$, i.e., $\rho = 0$. It is easy to integrate equation (A10) by parts in this case, and the central value of β turns out to be just the ratio of mean density to central density. On the other hand, $\alpha = \text{const}$ gives $\beta = 1$ throughout. The truth lies somewhere in between, with $\alpha \sim \text{const}$ near the center and $\alpha \sim r^3$ in the outer layers.

REFERENCES

- Alexander, M. E. 1973, *Ap&SS*, 23, 459
 Bell, J. F., Bessell, M. S., Stappers, B. W., Bailes, M., & Kaspi, V. M. 1995, *ApJ*, 447, L117
 Claret, A., & Giménez, A. 1993, *A&A*, 277, 487
 Eggleton, P. P. 2000, *NewA Rev.*, 44, 111
 ———. 2001, in *ASP Conf. Ser. 229, Evolution of Binary and Multiple Star Systems*, ed. Ph. Podsiadlowski, S. Rappaport, A. R. King, F. D'Antona, & L. Burderi, (San Francisco: ASP), 157
 Eggleton, P. P., Kiseleva, L. G., & Hut, P. 1998, *ApJ*, 499, 853 (EKH98)
 Guinan, E. F., Marshall, J. J., & Maloney, D. 1994, *Inf. Bull. Variable Stars*, 4101, 1
 Hut, P. 1981, *A&A*, 99, 126
 Iben, I., Jr., & Tutukov, A. V. 1998, *ApJ*, 501, 263 (IT98)
 Kaspi, V. M., Bailes, M., Manchester, R. N., Stappers, B. W., & Bell, J. F. 1996, *Nature*, 381, 584
 Kaspi, V. M., Johnston, S., Bell, J. F., Manchester, R. N., Bailes, M., Bessell, M., Lyne, A. G., & D'Amico, N. 1994, *ApJ*, 423, L43
 Kiseleva, L. G., Eggleton, P. P., & Mikkola, S. 1998, *MNRAS*, 300, 292 (KEM98)
 Kozai, Y. 1962, *AJ*, 67, 591
 Lacy, C. H. S. 1998, *AJ*, 115, 801
 Lacy, C. H. S., Helt, B. E., & Vaz, L. P. R. 1999, *AJ*, 117, 541
 Lestrade, J.-F., Phillips, R. B., Hodges, M. W., & Preston, R. A. 1993, *ApJ*, 410, 808
 Mazeh, T., & Shaham, J. 1979, *A&A*, 77, 145
 Refsdal, S., Roth, M. L., & Weigert, A. 1974, *A&A*, 36, 113
 Schmutz, W., et al. 1997, *A&A*, 328, 219
 Söderhjelm, S. 1975, *A&A*, 42, 229
 Tokovinin, A. A. 1997, *A&AS*, 124, 75
 Torres, G., & Stefanik, R. P. 2000, *AJ*, 119, 1914 (TS00)
 van den Heuvel, E. P. J., & van Paradijs, J. 1997, *ApJ*, 483, 399 (HP97)
 Vogt, S., & Fekel, F. C. 1979, *ApJ*, 234, 958
 Witte, M., & Savonije, G. T. 1999, *A&A*, 350, 129
 Zahn, J.-P. 1977, *A&A*, 57, 383
 ———. 1978, *A&A*, 67, 162